運輸省港湾技術研究所

港湾技術研究所報告

REPORT OF
THE PORT AND HARBOUR RESEARCH INSTITUTE
MINISTRY OF TRANSPORT

VOL. 7 NO. 3 SEPT. 1968

NAGASE, YOKOSUKA, JAPAN

港湾技術研究所報告は第7巻第1号より年4回定期的に刊行する。ただし第1巻から第6巻および欧文編第1号から第15号までは下記のとおり不定期に刊行された。

報告の入手を希望する方は論文番号を明記して港湾技術研究所長に申し込んで下さい。

和 文 篇 (Japanese Edition)

Vol. 1. No. 1 (1963)
Vol. 2. Nos. 1～3 (1963～1964)
Vol. 3. Nos. 1～7 (1964)
Vol. 4. Nos. 1～11 (1965)
Vol. 5. Nos. 1～15 (1966)
Vol. 6. Nos. 1～8 (1967)

欧 文 篇 (English Edition)

Report Nos. 1～15 (1963～1967)

The Report of the Port and Harbour Research Institute is published quarterly, either in Japanese or in occidental languages. The title and synopsis are given both in Japanese and in occidental languages.

The report prior to the seventh volume were published in two series in Japanese and English as listed above.

The copies of the Report are distributed to the agencies interested on the basis of mutual exchange of technical publication.

Inquiries relating to the Report should be addressed to the director of the Institute specifying the numbers of papers in concern.

港湾技術研究所報告 (REPORT OF P.H.R.I.)

第7巻 第3号 (Vol. 7, No. 3), 1968年9月 (Sept. 1968)

目 次 (CONTENTS)

REPORT OF THE PORT AND
HARBOUR RESARCH INSTITUTE
Vol. 7 No. 3 (Sept. 1968)

1. "Apparent Coefficient of Partial Reflection of Finite Amplitude Waves"

Yoshimi GODA*,
Yoshiki ABE**

Synopsis

Although Healy's method based on small amplitude wave theory is commonly used for the measurment of reflection coefficient, a simple use of Healy's method for waves of large steepness against a structure of high reflectivity causes an underestimation of reflection coefficient and an overestimation of incident wave height. The theory of partial standing waves has been developed to the third order approximation in order to calculate the wave heights at nodes and anti-nodes accurately. The theory, for example, demonstrates the appearance of twice frequency oscillation at nodal points for the case of total reflection. The apparent coefficient of wave reflection was then obtained from the calculated values of maximum and minimum wave heights and compared with the actual value of reflection coefficient. Several diagrams which shows the relation between the apparent and actual coefficients of wave reflection have been prepared for the relative depth of h/L=0.08, 0.10, 0.12, 0.15, 0.20 and 1.0. The ratio of apparent to actual incident waves has also been shown in similar diagrams.

Experiments have been done at the relative depth of h/L=0.1 and 0.2 for the wave reflection from a vertical wall and energy dissipators of horizontal wire mesh screens. The decrease of apparent reflection coefficient with the increase of wave steepness was in good agreement with the results of calculation shown in the correction diagrams. With these diagrams, the laboratory data on wave reflection by means of Healy's method can be corrected so as to yield the actual values of reflection coefficient and incident wave height.

The present theory of third order wave interaction also indicates decreases in wavelengths and increases in wave heights for both the incident and reflected waves. The standing wave height is therefore a little larger than twice the height of incident waves.

* Chief of Wave Laboratory, Hydraulics Division
** Member of Wave Laboratory, Hydraulics Division

港湾技術研究所報告 (REPORT OF P.H.R.I.)

第7巻 第3号 (Vol. 7, No. 3), 1968年9月 (Sept. 1968)

目 次 (CONTENTS)

港湾技術研究所報告
第7巻 第3号 (1968. 9)

1. “有限振幅波の部分反射に伴なう見掛けの反射率について”

合田良実*・阿部淑輝**

要旨

反射率の測定には，微小振幅波の理論による Healy の方法が通常用いられる。しかしながら，波形勾配の大きな波が構造物によって顕著に反射されているような場合に Healy の方法を単純に適用すると，見掛け上反射率が小さくなり，入射波高を過大に見積ることになる。このため，有限振幅の部分重複波を第3次近似まで計算し，重複波の節および腹における波高を正確に算定することとした。この計算によって，たとえば完全反射の場合には節の位置に2倍周波数の振動が出現することが明らかに示される。この節および腹における最小，最大波高から見掛けの反射率を求め，実際の反射率と比較し，この結果を水深波長比 h/L=0.08, 0.10, 0.12, 0.15, 0.20 および 1.0 ごとに図表化して示した。見掛けの入射波高比についても同様の図表を作成してある。

実験は，直立壁からの完全反射および水平金網型の消波装置からの部分反射について，水深波長比が h/L=0.1 および 0.2 の場合について行なった。波形勾配の増加に伴なう見掛けの反射率の減少は，上記図表の計算結果に一致した。したがって，これらの図表を用いれば，Healy の方法で算定した実験値を補正して，反射率および入射波高の実際の値を求めることが可能である。

また，この波の3次干渉の計算によると，入射波および反射波とも，波長が減少し，波高が増大することが示される。したがって重複波の波高は入射波高の2倍よりもやや大きくなる。

* 水工部 波浪研究室長
** 水工部 波浪研究室

CONTENTS

1. Introduction

The reflection of water waves is associated with every problem of wave and structure interaction. The intensity of wave reflection is a good index to the extent of interaction. For harbor engineers, the wave reflection inside a harbor basin is a source of trouble against the calmness of water basin. For coastal engineers, the waves reflected from a neighboring jetty is a possible cause of beach erosion.

All the problems related to the phenomenon of wave reflection require the data of reflection coefficient, or the ratio of reflected to incident wave heights. In certain problems such as a fixed thin board on the water surface, the reflection coefficient has been calculated theoretically[1]. In the problems involving the dissipation of wave energy, which apply for most of actual structures, the reflection coefficient cannot be predicted analytically but must be measured experimentally. By this reason many tests on the reflection coefficient have been done for various structures by means of scale models or for some generalized models. The experiments by Healy[2] and Greslou and Mahe[3] on uniform slopes belong to the latter group of laboratory study.

In most of wave tests, the reflection coefficient is determined by Healy's method which is based on the theory of small amplitude waves. According to this method, the wave height envelope of wave system in front of a test structure is measured, and the incident and reflected wave heights, H_I and H_R are estimated by the following formula from the data of maximum and minimum wave heights:

$$\left.\begin{aligned} H_I &= \frac{1}{2}(H_{\max}+H_{\min}) \\ H_R &= \frac{1}{2}(H_{\max}-H_{\min}). \end{aligned}\right\} \qquad (1)$$

The reflction coefficient is therefore obtained as

$$K_R=\frac{H_R}{H_I}=\frac{H_{\max}-H_{\min}}{H_{\max}+H_{\min}}. \qquad (2)$$

Although Healy's method is simple and convenient for use, it must be noted that the method is only that of first order approximation and must be employed with caution. Healy's method, for example, will give a reflection coefficient far below 1.0 for the case of total reflection ($K_R=1.0$) for the waves of large steepness in relatively shallow water, even though no wave energy is being dissipated[4]. Such the apparent decrease of reflection coefficient comes from the presence of higher order terms neglected in the small amplitude wave theory. Greslou and Mahe[3] have reported that the reflection coefficient of a steep slope gradually decreases as the wave steepness increases. This decrease also seems to be apparent one, because they employed Eqs. 1 and 2 for the determination of reflection coefficient.

The way to avoid the underestimation of reflection coefficient is either the direct measurement of reflected waves or the development of new method based on the wave theory of higher order approximation. Recently Murota and Yamada[5]

have introduced a method for direct recording of reflected waves. Using this method they have shown that a uniform slope steeper than 30 degree of angle has the reflection coefficient of 1.0 regardless of wave steepness. The method, however, is shown to be valid to the second order of approximation (see Section 3.4). In this report, the approach is taken toward the preparation of correction diagrams for Healy's method, taking the finite amplitude effect into consideration. One diagram for the case of total reflection in the intermediate depth has been given by one of the authors[4]. Another diagram for deep water waves has been sketched by James[6]. The present approach is based on the theory of third order wave interaction in the intermediate depth. The development of theory will be introduced in Chapter 2, and the calculation of apparent reflection coefficient as well as the correction diagrams will be shown in Chapter 3. The result of calculation will then be compared with the data of experiment conducted for that purpose in Chapter 4.

2. Theory of Finite Amplitude Waves

2.1 Progressive Waves

(1) Perturbed equations of the problem

The problem of finite amplitude wave of permanent type has been investigated by many researchers. If the problem is limited to the shallow water waves, the theory of cnoidal waves or solitary wave is available. If the problem is concerned with surface waves in the intermediate depth, the theory of Stokes waves which expresses the velocity potential and surface profile in terms of harmonic series is employed. At present the fifth order theory has been calculated by Skjelbreia and Hendrickson[7]. Numerical computations of higher order approximation have been demonstrated by Chappelear[8] and Dean[9]. Though the theory of finite amplitude progressive waves is well established, the calculation of third order theory by means of perturbation method will be shown in this section as the preparation for the calculation of partial standing waves. The procedure is analoguous to that for standing waves calculated by Tadjbaksh and Keller[10].

As usual, the viscosity of water is considered as negligible and the motion is treated as irrotational. Thus, the velocity potential Φ must satisfy the Laplace equation of

$$\Phi_{xx}+\Phi_{yy}=0, \tag{3}$$

where x is the horizontal coordinate and y is the vertical coordinate measured upward from the still water level. In this study, only the two dimensional motion will be treated. With the velocity potential Φ, the particle velocities, u and v, are expressed as Φ_x and Φ_y, respectively. At the water surface, the pressure must be zero and the water particle consistituting the surface must remain there throughout the motion. These conditioned are described as

$$g\eta+\Phi_t+\frac{1}{2}(\Phi_x^2+\Phi_y^2)=0 \qquad \text{on} \quad y=\eta \tag{4}$$

$$\Phi_y=\eta_t+\eta_x\Phi_x \qquad \text{on} \quad y=\eta, \tag{5}$$

in which η is the vertical displacement of the water surface measured from $y=0$. For the water of uniform depth of h, the boundatary condition is

$$\Phi_y=0 \qquad \text{on} \quad y=-h. \tag{6}$$

In addition, the conservation of water mass requires the average water level must be at $y=0$, and the motion must be periodic both in x and t. These conditions are

$$\int_0^{2\pi/k}\eta(x,t)\,dx=0 \tag{7}$$

$$\nabla\Phi(x,y,t+2\pi/\sigma)=\nabla\Phi(x+2\pi/k,y,t)=\nabla\Phi(x,y,t), \tag{8}$$

in which k is the wave number and σ is the angular frequency. Further, the solution of progressive waves travelling toward the positive direction of x will be sought.

Since Eqs. 4 and 5 are nonlinear, the following pertubated solutions with a parameter of small quantity a are assumed here for Φ, η and σ.

$$\left.\begin{aligned}
&\Phi(x,y,t)=a\Phi^{(0)}(x,y,t)+a^2\Phi^{(1)}(x,y,t)+\frac{1}{2}a^3\Phi^{(2)}(x,y,t)+O(a^4)\\
&\eta(x,t)=a\eta^{(0)}(x,t)+a^2\eta^{(1)}(x,t)+\frac{1}{2}a^3\eta^{(2)}(x,t)+O(a^4)\\
&\sigma=\sigma_0+a\sigma_1+\frac{1}{2}a^2\sigma_2+O(a^3).
\end{aligned}\right\} \tag{9}$$

Equations 4 and 5 are rewritten with Eq. 9 for the conditions at $y=0$ instead of $y=\eta$. Resultant equations are arranged with the terms of equal powers of a to yield the following sets of perturbed equations for the surface conditions:

$$g\eta^{(0)}+\sigma_0\Phi_\tau^{(0)}=0 \tag{4^1}$$

$$g\eta^{(1)}+\sigma_0\Phi_\tau^{(1)}+\sigma_1\Phi_\tau^{(0)}=-\sigma_0\eta^{(0)}\Phi_{\tau y}^{(0)}-\frac{1}{2}[\Phi_x^{(0)2}+\Phi_y^{(0)2}] \tag{4^2}$$

$$\begin{aligned}
\frac{1}{2}g\eta^{(2)}+\frac{1}{2}\sigma_0\Phi_\tau^{(2)}+\frac{1}{2}\sigma_2\Phi_\tau^{(2)}=&-\sigma_1\eta^{(0)}\Phi_{\tau y}^{(0)}-\sigma_0\eta^{(1)}\Phi_{\tau y}^{(0)}-\sigma_0\eta^{(0)}\Phi_{\tau y}^{(1)}\\
&-\frac{1}{2}\sigma_0\eta^{(0)2}\Phi_{\tau yy}^{(0)}-\eta^{(0)}[\Phi_x^{(0)}\Phi_{xy}^{(0)}+\Phi_y^{(0)}\Phi_{yy}^{(0)}]\\
&-\Phi_x^{(0)}\Phi_x^{(1)}-\Phi_y^{(0)}\Phi_y^{(1)}\\
&\text{on} \quad y=0,
\end{aligned} \tag{4^3}$$

and

$$\Phi_y^{(0)}-\sigma_0\eta_\tau^{(0)}=0 \tag{5^1}$$

$$\Phi_y^{(1)}-\sigma_0\eta_\tau^{(1)}-\sigma_1\eta_\tau^{(0)}=-\eta^{(0)}\Phi_{yy}^{(0)}+\eta_x^{(0)}\Phi_x^{(0)} \tag{5^2}$$

$$\begin{aligned}
\frac{1}{2}\Phi_y^{(2)}-\frac{1}{2}\sigma_0\eta_\tau^{(2)}-\sigma_1\eta_\tau^{(1)}-\frac{1}{2}\sigma_2\eta_\tau^{(0)}=&-\eta^{(1)}\Phi_{yy}^{(0)}-\frac{1}{2}\eta^{(0)2}\Phi_{yyy}^{(0)}\\
&-y^{(0)}\Phi_{yy}^{(1)}+\eta_x^{(0)}\eta^{(0)}\Phi_{xy}^{(0)}+\eta_x^{(0)}\Phi_x^{(1)}+\eta_x^{(1)}\Phi_x^{(0)}\\
&\text{on} \quad y=0,
\end{aligned} \tag{5^3}$$

where τ is the non-dimensional time of the following:

$$\tau=\sigma t=\left(\sigma_0+a\sigma_1+\frac{1}{2}a^2\sigma_2+\cdots\right)t. \tag{10}$$

The rest of equations, Eqs. 3, 6, 7 and 8 are linear; hence they are applied to each perturbed solutions of Φ and η, i.e., $\Phi^{(0)}$, $\Phi^{(1)}$, $\Phi^{(2)}$,$\cdots$ and $\eta^{(0)}$, $\eta^{(1)}$, $\eta^{(2)}$,$\cdots$

(2) First order solution

The general solution of Eq. 3 which also satisfies the bottom and periodicity conditions of Eqs. 6 and 8 is written as

$$\Phi^{(r)}(x, y, t)=\sum_{n=0}^{\infty}[A_n^{(r)}(t)\sin nkx+B_n^{(r)}(t)\cos nkx]\cosh nk(y+h), \tag{11}$$

with the condition of

$$\left.\begin{aligned}&A_n^{(r)}(t+2\pi/\sigma)=A_n^{(r)}(t)\\&B_n^{(r)}(t+2\pi/\sigma)=B_n^{(r)}(t),\end{aligned}\right\} \tag{12}$$

in which r is an integer of 0, 1 or 2.

In order to solve $A_n^{(0)}(t)$ and $B_n^{(0)}(t)$, the surface conditions of Eqs. 4^1 and 5^1 are combined to yield

$$g\Phi_y^{(0)}+\sigma_0^2\Phi_{\tau\tau}^{(0)}=0 \qquad \text{on} \quad y=0. \tag{13}$$

The substitution of Eq. 11 into Eq. 13 results in

$$ngk\begin{Bmatrix}A_n^{(0)}\\B_n^{(0)}\end{Bmatrix}\sinh nkh+\sigma_0^2\begin{Bmatrix}A_{n_{\tau\tau}}^{(0)}\\B_{n_{\tau\tau}}^{(0)}\end{Bmatrix}\cosh nkh=0 \quad \text{with} \quad n=0,1,2,\cdots \tag{14}$$

From the terms for $n=0$, $B_0^{(0)}$ is obtained as

$$B_0^{(0)}=\alpha_0\tau+\beta_0. \tag{15}$$

From the terms for $n\geq 2$, the condition of Eq. 12 with the relation of Eq. 17 yield $A_n(\tau)=B_n(\tau)=0$.

From the terms for $n=1$, the equation for $A_1^{(0)}$ and $B_1^{(0)}$ are derived as

$$\frac{A_{1_{\tau\tau}}^{(0)}}{A_1^{(0)}}=\frac{B_{1_{\tau\tau}}^{(0)}}{B_1^{(0)}}=-\frac{1}{\sigma_0^2}gk\tanh kh. \tag{16}$$

Since $A_1^{(0)}(\tau)$ and $B_1^{(0)}(\tau)$ must be periodic funtions with the period of 2π, σ_0 is required to satisfy the following relation:

$$\sigma_0^2=gk\tanh kh. \tag{17}$$

With the above relation, $A_1^{(0)}$ and $B_1^{(0)}$ are obtained as the sum of $\sin\tau$ and $\cos\tau$ with arbitrary coefficients. Therefore, the first order solution of velocity potential $\Phi^{(0)}$ is wirtten as

$$\Phi^{(0)}=\alpha_0\tau+\beta_0+[(\alpha_1\sin\tau+\beta_1\cos\tau)\sin kx$$
$$+(\alpha^2\sin\tau+\beta_2\cos\tau)\cos kx]\cosh k(y+h). \tag{18}$$

Since we are interested in progressive waves only, we take the following form for $\Phi^{(0)}$:

$$\Phi^{(0)}=\alpha_0\tau+\beta_0+\alpha_1'\sin(kx-\tau)\cosh k(y+h). \tag{19}$$

The surface displacement η is then obtained by substituting Eq. 18 into Eq. 1 as

$$\eta^{(0)}=\frac{\sigma_0}{g}[-\alpha_0+\alpha_1'\cos(kx-\tau)\cosh kh]. \tag{20}$$

Now the application of Eq. 7 results in $\alpha_0=0$. If the first order amplitude of surface displacement is set to a, then the amplitude of $\eta^{(0)}$ must be unity; hence

$$\alpha_1'=\frac{\sigma_0}{k\sinh kh}. \tag{21}$$

Thus the first order solution of $\Phi^{(0)}$, $\eta^{(0)}$, and σ_0 are written as

$$\left.\begin{aligned}\Phi^{(0)}&=\frac{\sigma_0}{k}\sin(kx-\sigma t)\frac{\cosh k(y+h)}{\sinh kh}\\ \eta^{(0)}&=\cos(kx-\sigma t)\\ \sigma_0^2&=gk\tanh kh.\end{aligned}\right\} \tag{22}$$

(3) The second order solution

The result of Eq. 22 is substituted into Eqs. 4^2 and 5^2 in order to obtain the following surface conditions for the second order solution:

$$g\eta^{(1)}+\sigma_0\Phi_\tau^{(1)}-\frac{\sigma_1}{\sigma_0}g\cos(kx-\tau)$$
$$=-\frac{1}{4}\sigma_0^2(\coth^2 kh-3)\cos 2(kx-\tau)$$
$$-\frac{1}{4}\sigma_0^2(\coth^2 kh-1)\qquad\text{on}\quad y=0 \tag{23}$$

$$\Phi_y^{(1)}-\sigma_0\eta_\tau^{(0)}-\sigma_1\sin(kx-\tau)=-\sigma_0 k\coth kh\sin 2(kx-\tau)\quad\text{on}\quad y=0. \tag{24}$$

The term of $\eta^{(1)}$ can be eliminated from the above as in the following:

$$g\Phi_y^{(1)}+\sigma_0^2\Phi_{\tau\tau}^{(1)}=2gk\sigma_1\sin(kx-\tau)$$
$$-\frac{3}{2}\sigma_0^3(\coth^2 kh-1)\sin 2(kx-\tau)\qquad\text{on}\quad y=0. \tag{25}$$

Since the general solution for $\Phi^{(1)}$ is given with Eq. 11, the substitution of this equation into the above yields the following set of equations for $A_n^{(1)}$ and $B_n^{(1)}$:

$$B_{0_{\tau\tau}}^{(1)}=0 \tag{26}$$

$$gk\begin{Bmatrix} A_1^{(1)} \\ B_1^{(1)} \end{Bmatrix} \sinh kh+\sigma_0^2\begin{Bmatrix} A_{1_{\tau\tau}}^{(1)} \\ B_{1_{\tau\tau}}^{(1)} \end{Bmatrix} \cosh kh=2gk\sigma_1\begin{Bmatrix} \cos\tau \\ -\sin\tau \end{Bmatrix}. \tag{27}$$

$$2gk\begin{Bmatrix} A_2^{(1)} \\ B_2^{(1)} \end{Bmatrix} \sinh 2kh+\sigma_0^2\begin{Bmatrix} A_{2_{\tau\tau}}^{(1)} \\ B_{2_{\tau\tau}}^{(1)} \end{Bmatrix}\cosh 2kh$$

$$=-\frac{3}{2}\sigma_0^3(\coth^2 kh-1)\begin{Bmatrix} \cos 2\tau \\ -\sin 2\tau \end{Bmatrix} \tag{28}$$

$$ngk\begin{Bmatrix} A_n^{(1)} \\ B_n^{(1)} \end{Bmatrix} \sinh nkh+\sigma_0^2\begin{Bmatrix} A_{n_{\tau\tau}}^{(1)} \\ B_{n_{\tau\tau}}^{(1)} \end{Bmatrix} \cosh nkh=0 \qquad \text{for} \quad n\geq 3. \tag{29}$$

The first equation gives

$$B_0^{(1)}=\alpha_{01}\tau+\beta_{01}. \tag{30}$$

The second equation is rewritten with the relation of Eq. 17 as

$$\begin{Bmatrix} A_1^{(1)} \\ B_1^{(1)} \end{Bmatrix}+\begin{Bmatrix} A_{1_{\tau\tau}}^{(1)} \\ B_{1_{\tau\tau}}^{(1)} \end{Bmatrix}=\frac{2\sigma_1}{\sinh kh}\begin{Bmatrix} \cos\tau \\ -\sin\tau \end{Bmatrix}. \tag{31}$$

The condition of Eq. 12 now requires $A_1^{(1)}(\tau)$ and $B_1^{(1)}(\tau)$ to be harmonic functions with the period of $2\pi/m$ where m is an integer of 1, 2, 3,$\cdots$.; the right-hand side of the above equation then requires the period to be 2π. Hence,

$$\begin{Bmatrix} A_1^{(1)} \\ B_1^{(1)} \end{Bmatrix}=\begin{Bmatrix} \alpha_1 \\ \alpha_2 \end{Bmatrix} \sin\tau+\begin{Bmatrix} B_1 \\ B_2 \end{Bmatrix} \cos\tau. \tag{32}$$

The substitution of Eq. 32 into Eq. 31 leaves the left-hand side of the latter in zero; hence the term of σ_1 must be zero:

$$\sigma_1=0. \tag{33}$$

Equation 28 for $A_2^{(1)}$ and $B_2^{(1)}$ can be solved easily as

$$\begin{Bmatrix} A_2^{(1)} \\ B_2^{(1)} \end{Bmatrix}=\frac{3}{8}\sigma_0\frac{\coth^4 kh-1}{\cosh 2kh}\begin{Bmatrix} \cos 2\tau \\ -\sin 2\tau \end{Bmatrix}. \tag{34}$$

For $n\geq 3$, $A_n^{(1)}$ and $B_n^{(1)}$ must be zero by Eq. 29.

In the above solutions, the coefficient for $A_1^{(1)}$ and $B_1^{(1)}$ remained undetermined. The condition of progressive waves is then applied to eliminate three out of four coefficients. Thus $\Phi^{(1)}$ is obtained as

$$\Phi^{(1)}=\alpha_{01}\tau+\beta_{01}+\alpha_1'' \sin(kx-\tau)\cosh k(y+h)$$

$$+\frac{3}{8}\sigma_0(\coth^4 kh-1)\sin 2(kx-\tau)\frac{\cosh 2k(y+h)}{\cosh 2kh}. \tag{35}$$

The second order solution of surface displacement $\eta^{(1)}$ is then derived by substituting the above equation with Eq. 33 into Eq. 24 as

$$\eta^{(1)}=-\frac{\sigma_0}{g}\alpha_{01}-\frac{1}{4}\frac{\sigma_0^2}{g}(\coth^2 kh-1)+\frac{\sigma_0}{g}\alpha_1''\cosh kh\cos(kx-\tau)$$
$$+\frac{1}{4}k(3\coth^3 kh-\coth kh)\cos 2(kx-\tau). \tag{36}$$

The term of α_{01} is determined by the condition of Eq. 7 as

$$\alpha_{01}=-\frac{1}{4}\sigma_0(\coth^2 kh-1). \tag{37}$$

The term of β_{01} can be set to zero, since β_{01} merely adds a small change to the level of velocity potential which has already been given by the first order constant of β_0. The term of α_1'' can also be set to zero, since α_1'' represents the amplitude of arbitrarily superposed waves. Therefore, the second order solution of $\Phi^{(1)}$, $\eta^{(1)}$, and σ_1 become as follows:

$$\left.\begin{aligned}\Phi^{(1)}&=\sigma_0\alpha_{01}\tau+\sigma_0\beta_{22}\cos 2(kx-\tau)\cosh 2k(y+h)\\ \eta^{(1)}&=kb_{22}\cos 2(kx-\tau)\\ \sigma_1&=0,\end{aligned}\right\} \tag{38}$$

where:

$$\left.\begin{aligned}\alpha_{01}&=-\frac{1}{4}(\coth^2 kh-1)\\ \beta_{22}&=\frac{3}{8}\frac{(\coth^4 kh-1)}{\cosh 2kh}\\ b_{22}&=\frac{1}{4}(3\coth^3 kh-\coth kh).\end{aligned}\right\} \tag{39}$$

(4) Third order solution

The general solution of $\Phi^{(2)}$ is given by Eq. 11 as well as for $\Phi^{(0)}$ and $\Phi^{(1)}$. The equations for the determination of $A_n^{(2)}$ and $B_n^{(2)}$ are obtained from the second order perturbation of surface conditions, Eqs. 4[3] and 5[3] with Eqs. 22 and 38 being substituted into them. After some manipulation, they are rewritten as

$$g\eta^{(2)}+\sigma_0\Phi_\tau^{(2)}-\frac{\sigma_2}{\sigma_0}g\cos(kx-\tau)$$
$$=\frac{3}{4}k\sigma_0^2(-c^5+3c^3-3c)\cos(kx-\tau)$$
$$+\frac{3}{4}k\sigma_0^2(-c^5+7c^3-5c)\cos 3(kx-\tau)\qquad\text{on}\quad y=0, \tag{40}$$

and

$$\Phi_y^{(2)}-\sigma_0\eta_\tau^{(2)}-\sigma_2\cos(kx-\tau)$$
$$=\frac{1}{4}k^2\sigma_0(-6c^4+c^2)\sin(kx-\tau)$$
$$+\frac{3}{4}k^2\sigma_0(-6c^4+c^2+2)\sin 3(kx-\tau)\qquad\text{on}\quad y=0, \tag{41}$$

where:

$$c=\coth kh. \tag{42}$$

From Eqs. 40 and 41, the terms of $\eta^{(2)}$ are eliminated to yield the equation for $\Phi^{(2)}$ as

$$g\Phi_y^{(2)}+\sigma_0^2\Phi_{\tau\tau}^{(2)}=g\left[2\sigma_2+\frac{1}{4}k^2\sigma_0(-9c^4+10c^2-9)\sin(kx-\tau)\right]$$
$$+\frac{3}{4}gk^3\sigma_0(-9c^4+22c^2-13)\sin 3(kx-\tau) \quad \text{on} \quad y=0. \tag{43}$$

As in the preceding sections, the equations for $A_n^{(2)}$ and $B_n^{(2)}$ are easily obtained by substituting Eq. 11 into the above and by assembling the terms with equal value of n as

$$B_{0_{\tau\tau}}^{(2)}=0 \tag{44}$$

$$gk\begin{Bmatrix}A_1^{(2)}\\B_1^{(2)}\end{Bmatrix}\sinh kh+\sigma_0^2\begin{Bmatrix}A_{1_{\tau\tau}}^{(2)}\\B_{1_{\tau\tau}}^{(2)}\end{Bmatrix}\cosh kh$$
$$=g\left[2\sigma_2+\frac{1}{4}k^2\sigma_0(-9c^4+10c^2-9)\right]\begin{Bmatrix}\cos\tau\\-\sin\tau\end{Bmatrix} \tag{45}$$

$$3gk\begin{Bmatrix}A_3^{(2)}\\B_3^{(2)}\end{Bmatrix}\sinh 3kh+\sigma_0^2\begin{Bmatrix}A_{3_{\tau\tau}}^{(2)}\\B_{3_{\tau\tau}}^{(2)}\end{Bmatrix}\cosh 3kh$$
$$=\frac{3}{4}gk^3\sigma_0(-9c^4+22c^2-13)\begin{Bmatrix}\cos 3\tau\\-\sin 3\tau\end{Bmatrix} \tag{46}$$

$$ngk\begin{Bmatrix}A_n^{(2)}\\B_n^{(2)}\end{Bmatrix}\sinh nkh+\sigma_0^2\begin{Bmatrix}A_{n_{\tau\tau}}^{(2)}\\B_{n_{\tau\tau}}^{(2)}\end{Bmatrix}\cosh nkh=0 \quad \text{for} \quad n=2 \text{ and } n\geq 4. \tag{47}$$

Although the first equation of the above yields the solution of $B_0^{(2)}=\alpha_{02}\tau+\beta_{02}$, the coefficient of α_{02} is shown to be zero by the condition of Eq. 7 and β_{02} can be set to zero by being included into β_0; hence, $B_0^{(2)}=0$. Next for the second equation, the periodic condition of Eq. 12 results in nulifying the coefficient of the right-hand side. This determines σ_2 as

$$\sigma_2=-\frac{1}{8}k^2\sigma_0(-9c^4+10c^2-9). \tag{48}$$

The functions of $A_1^{(2)}(\tau)$ and $B_1^{(2)}(\tau)$ can be taken as arbitrary combinations of $\sin\tau$ and $\cos\tau$. But the condition of progressive waves requires the following form with an undetermined coefficient of α_2:

$$A_1^{(2)}(\tau)=\alpha_2\cos\tau, \quad \text{and} \quad B_1^{(2)}(\tau)=-\alpha_2\sin\tau. \tag{49}$$

The functions of $A_3^{(2)}$ and $B_3^{(2)}$ are uniquely determined by Eq. 46, and the functions of $A_n^{(2)}$ and $B_n^{(2)}$ for $n=2$ and $n\geq 4$ are lead to zero by Eq. 47.

The third order solution of velocity potential $\Phi^{(3)}$ is thus obtained as:

$$\Phi^{(3)}=\alpha_3 \sin(kx-\tau)\cosh k(y+h)$$
$$+\frac{1}{32}k\sigma_0(c^3+3)(9c^5-22c^3+13c)\sin 3(kx-\tau)\frac{\cosh 3k(y+h)}{\cosh 3kh}. \tag{50}$$

The first term of the right-hand side expresses an progressive wave superposed to the system in question. Although the assignment of a specific value to the amplitude α_3 is arbitrary, α_3 is taken to be zero in this report, because the situation is simplified by this and the solution can be directly compared with that of finite amplitude standing waves.

The third order solution of surface displacement $\eta^{(3)}$ is then calculated by substituting Eq. 50 with $\alpha_3=0$ into Eq. 40. Thus the final results of $\Phi^{(3)}$, $\eta^{(3)}$, and σ_3 become

$$\left.\begin{aligned}&\Phi^{(3)}=k\sigma_0\beta_{33}\sin 3(kx-\tau)\cosh 3k(y+h)\\&\eta^{(3)}=k^2\{b_{11}\cos(kx-\tau)+b_{33}\cos 3(kx-\tau)\}\\&\sigma_3=k^2\sigma_0 C_1,\end{aligned}\right\} \tag{51}$$

where:

$$\left.\begin{aligned}&\beta_{33}=\frac{1}{32\cosh^3 kh}(c^2+3)(9c^5-22c^3+13c)\\&b_{11}=\frac{1}{8}(3c^4+8c^2-9)\\&b_{33}=\frac{3}{32}(9c^6-3c^4+3c^2-1)\\&C_1=\frac{1}{8}(9c^4-10c^2+9)\end{aligned}\right\} \tag{52}$$

(5) Wave height and wavelength of progressive waves

Summing up the above results, the perturbed solution of progressive waves to the third approximation is written as

$$\left.\begin{aligned}&\frac{k^2}{\sigma_0}\Phi=\varepsilon\beta_{11}\sin(kx-\sigma t)\cosh k(y+h)+\varepsilon^2\alpha_{01}\sigma t\\&\qquad+\varepsilon^2\beta_{22}\sin 2(kx-\sigma t)\cosh 2k(y+h)\\&\qquad+\frac{1}{2}\varepsilon^3\beta_{33}\sin 3(kx-\sigma t)\cosh 3k(y+h)\\&k\eta=\left[\varepsilon+\frac{1}{2}\varepsilon^3 b_{11}\right]\cos(kx-\sigma t)+\varepsilon^2 b_{22}\cos 2(kx-\sigma t)\\&\qquad+\frac{1}{2}\varepsilon^3 b_{33}\cos 3(kx-\sigma t)\\&\sigma=\sigma_0\left[1+\frac{1}{2}\varepsilon^2 C_1\right].\end{aligned}\right\} \tag{53}$$

where:

$$\left.\begin{aligned}\varepsilon&=ka\\ \beta_{11}&=1/\sinh kh\end{aligned}\right\} \tag{54}$$

The parameter ε is related to the wave height H as

$$kH=2\varepsilon+\varepsilon^3(b_{11}+b_{33}). \tag{55}$$

So far the solution has been obtained with the fixed value of wave number k in search of angular frequency which satisfies the relation between k, h and ε. If the angular frequency is given *a priori* as in the case of mechanically generated waves, the wave number k will very with ε. The variation of wave number can be calculated by the following relation which has been obtained from Eqs. 17 and 54:

$$\sigma^2=gk\tanh kh\left[1+\frac{1}{2}\varepsilon^2 C_1\right]^2 \tag{56}$$

We can also define a wave number k_A of the following as the first order approximation to wave number:

$$\sigma^2=gk_A\tanh k_Ah \tag{57}$$

The wave number k is now related to the first order approximation k_A as

$$kh\tanh kh\left[1+\frac{1}{2}\varepsilon^2 C_1\right]^2=k_Ah\tanh k_Ah. \tag{58}$$

By taking the terms of up to ε^2, the relation between k and k_A is approximated to the third order as

$$k=k_A\left[1-\frac{1}{2}\varepsilon^2 K_1\right], \tag{59}$$

where:

$$K_1=\frac{2C_1}{1+k_Ah(\coth k_Ah-\tanh k_Ah)}. \tag{60}$$

Thus the wave number of finite amplitude progressive waves is shown to decrease with the increase of amplitude; the wavelength increases.

In comparison with the solution by Skjelbreia and Hendrickson[7], the present solution does not have the term of $\varepsilon^3A_{13}\sin(kx-\sigma t)\cosh k(y+h)$ in the expression for Φ while the term of $\varepsilon^3b_{11}\cos(kx-\sigma t)$ appears in η instead. This difference comes from the assignment of a value to α_2 in Eq. 50. Skjelbreia and Hendrickson have so chosen that the amplitude of fundamental harmonic of the surface displacement is given by a, though they have obtained the solution by assuming the surface displacement to be a form of $\sum_{n=1}^{\infty}\varepsilon^n b_{nn}\cos n(kx-\sigma t)$ *a priori*. Becarse of this difference, the value of ε for a given wave height is different in their solution from the present one. Another difference is the absence of α_{01} term in their solution, which has a correction to the constant of Bernouille equation instead.

Other coefficients are shown to be the same with the corresponding ones in

their solution and present one, after some manupilation with hyperbolic functions. The phase velocity of σ/k is also shown to agree each other to the order of second power of ε. Therefore, the present solution is another expression of finite amplitude progressive waves to the third order approximation.

2.2 Partial Standing Waves

(1) Perturbation of partial standing waves

When two trains of finite amplitude waves interact each other, the surface conditions of Eqs. 4 and 5 cannot be satisfied by a simple superposition of two waves only. Because of non-linearity of the equations, some bound waves are required to appear. The situation can be considered in such a way that the original two waves deform themselves by the result of interaction and the difference due to deformation is expressed as bound waves. This property of finite amplitude waves has been clearly shown by Hamada[11] in the calculation of second order interaction.

The phenomenon of partial standing waves produced by partial reflection is a typical example of wave interaction which produces bound waves. The perturbed solution of partual standing waves, therefore, must be composed of progressive waves, retrogressive waves, and bound waves. In this report the perturbed solution of bound waves will be sought under the condition of progressive and retrogressive waves of finite amplitudes being given independently. Thus the expressions for the velocity potential and surface displacement will have the following form of perturbation:

$$\left.\begin{aligned} &\Phi=\Phi_I+\Phi_R+\Phi_F,\\ &\text{where:}\quad \Phi_I=a\Phi_I^{(0)}+a^2\Phi_I^{(1)}+\frac{1}{2}a^3\Phi_I^{(2)}\\ &\qquad\quad \Phi_R=\lambda a\Phi_R^{(0)}+\lambda^2 a^2\Phi_R^{(1)}+\frac{1}{2}\lambda^3 a^3\Phi_R^{(2)}\\ &\qquad\quad \Phi_F=a^2\Phi_F^{(1)}+\frac{1}{2}a^3\Phi_F^{(2)}, \end{aligned}\right\} \tag{61}$$

and

$$\left.\begin{aligned} &\eta=\eta_I+\eta_R+\eta_F,\\ &\text{where:}\quad \eta_I=a\eta_I^{(0)}+a^2\eta_I^{(1)}+\frac{1}{2}a^3\eta_I^{(2)}\\ &\qquad\quad \eta_R=\lambda a\eta_R^{(0)}+\lambda^2 a^2\eta_R^{(1)}+\frac{1}{2}\lambda^3 a^3\eta_R^{(2)}\\ &\qquad\quad \eta_F=a^2\eta_F^{(1)}+\frac{1}{2}a^3\eta_F^{(2)}, \end{aligned}\right\} \tag{62}$$

in which the subscripts, I, R and F deonte the progressive, retrogressive, and bound waves, respectively. The factor λ represents the ratio of retrogressive to progressive wave amplitudes in the first order approximation. The pertubed solutions of progressive and retrogressive waves, $\Phi_I^{(r)}$, $\Phi_R^{(r)}$, $\eta_I^{(r)}$, $\eta_R^{(r)}$ where $r=0$, 1 and 2 are given by Eqs. 22, 38 and 51 with the wave number of k_I and k_R

respectively; for retrogressive waves, k_R takes a negative value.

The perturbation for angular frequency needs a special treatment. As shown in Eq. 52, the angular frequency for a given wave number increases as the wave amplitude increases. This can be interpreted as the increase in wavelength for a given wave period. In case of partial standing waves produced by wave reflection, no change in wave period will take place as deduced from the physical situation; the wavelength must change instead of wave period if any change takes place. The perturbation of wave number is troublesome, however, since the wave number appears explicitly in the surface condition whenever the derivative with respect to x or y is taken. Therefore, the angular frequency of progressive and retrogressive waves are perturbed in this report in order to obtain the correction terms, and then the equality of wave frequency will be introduced so as to yield the change in wave number. Taking the results of progressive waves into consideration, the perturbations of angular frequencies are expressed as

$$\left.\begin{aligned}\sigma_I&=\sigma_0+\frac{1}{2}a^2(\sigma_2+\sigma_{IF})\\ \sigma_R&=\sigma_0+\frac{1}{2}a^2(\lambda^2\sigma_2+\sigma_{RF}).\end{aligned}\right\} \tag{63}$$

The first and third order perturbed frequencies of σ_0 and σ_2 are given by Eqs. 17 and 48, respectively.

(2) Second order solution of bound waves

The perturbed solution of partial standing waves expressed by Eqs. 61, 62 and 63 must satisfy Eqs. 3 through 7. The periodicity condition of Eq. 8 is applied with due regard to the wave number and angular frequency of bound waves, which will be expressed as the sum or difference of the multiples of k_I, k_R, σ_I and σ_R.

The general solution of Φ_F is immediately obtained from the linear equations of 3, 6 and 8 in the same form with Eqs. 11 and 12, i.e.

$$\Phi_F^{(r)}(x, y, t)=\sum_{n=0}^{\infty}[A_n^{(r)}(t)\sin nk_Fx+B_n^{(r)}\cos nk_Fx]\times\cosh nk_F(y+h)\qquad\text{with}\quad r=1\text{ or }2, \tag{64}$$

with the condition of

$$\left.\begin{aligned}A_n^{(r)}(t+2\pi/\sigma_F)&=A_n^{(r)}(t)\\ B_n^{(r)}(t+2\pi/\sigma_F)&=B_n^{(r)}(t).\end{aligned}\right\} \tag{65}$$

The time functions $A_n^{(r)}(t)$ and $B_n^{(r)}(t)$ must be determined from the surface conditions of Eqs. 4 and 5, into which the expressions of Eqs. 61, 62 and 63 are introduced to yield the equations for bound waves. Since the group of terms with only $\Phi_I^{(r)}$, $\eta_I^{(r)}$ and their products satisfy the surface conditions by themselves as well as the group with $\Phi_R^{(r)}$ and $\eta_R^{(r)}$, the remaining terms with $\Phi_F^{(r)}$, $\eta_F^{(r)}$, and cross products of $\Phi_I^{(r)}$, $\Phi_R^{(r)}$, $\eta_I^{(r)}$ and $\eta_R^{(r)}$ become as follows for the second power of a:

$$g\eta_F^{(1)}+\Phi_{F_t}^{(1)}=-\lambda\sigma_0\eta_R^{(0)}\Phi_{I_{zy}}^{(0)}-\lambda\sigma_0\eta_I^{(0)}\Phi_{R_{zy}}^{(0)}-\lambda\Phi_{I_x}^{(0)}\Phi_{R_x}^{(0)}-\lambda\Phi_{I_y}^{(0)}\Phi_{R_y}^{(0)}\qquad\text{on}\quad y=0, \tag{66}$$

$$\Phi^{(1)}_{F_y}-\eta^{(1)}_{F_t}=\lambda\eta^{(0)}_{R_x}\Phi^{(0)}_{I_x}+\lambda\eta^{(0)}_{I_x}\Phi^{(0)}_{R_x}-\lambda\eta^{(0)}_{R}\Phi^{(0)}_{I_{yy}}-\lambda\eta^{(0)}_{I}\Phi^{(0)}_{R_{yy}} \quad \text{on} \quad y=0, \tag{67}$$

where:

$$\left.\begin{array}{ll} \tau=\sigma_I t & \text{for } \Phi_I \text{ and } \eta_I \\ \text{or} & \\ \tau=\sigma_R t & \text{for } \Phi_R \text{ and } \eta_R. \end{array}\right\} \tag{68}$$

The derivatives of Φ_F and η_F with respect to t will be calculated without resorting to non-dimensional time τ since the angular frequency σ_F is unknown at this stage.

The right-hand sides of Eqs. 66 and 67 are calculated after the substitution of the expressions for $\Phi^{(0)}_I$, $\Phi^{(0)}_R$, $\eta^{(0)}_I$ and $\eta^{(0)}_R$ which are given by Eq. 22 with the change of k into k_I or k_R. The results of calculation become

$$g\eta^{(1)}_F+\Phi^{(1)}_{F_t}=\frac{1}{2}\lambda\sigma_0^2[3-\coth(I)\coth(R)]\cos(I+R)$$
$$+\frac{1}{2}\lambda\sigma_0^2[1-\coth(I)\coth(R)]\cos(I-R) \quad \text{on} \quad y=0, \tag{69}$$

and

$$g\Phi^{(1)}_{F_y}-g\eta^{(1)}_{F_t}=-\frac{1}{2}\lambda\sigma_0^3[\coth(I)+\coth(R)]^2\sin(I+R)$$
$$-\frac{1}{2}\lambda\sigma_0^3[\coth^2(I)-\coth^2(R)]\sin(I-R) \quad \text{on} \quad y=0, \tag{70}$$

where:

$$\left.\begin{array}{l} \coth(I)=\coth k_I h \\ \coth(R)=\coth k_R h \\ \cos(I\pm R)=\cos[(k_I\pm k_R)x-(\sigma_I\pm\sigma_R)t] \\ \sin(I\pm R)=\sin[(k_I\pm k_R)x-(\sigma_I\pm\sigma_R)t]. \end{array}\right\} \tag{71}$$

The elimination of $\eta^{(1)}_F$ from the above equations results in

$$g\Phi^{(1)}_{F_y}+\Phi^{(1)}_{F_{tt}}=\lambda\sigma_0^3\{6-\coth^2(I)-\coth^2(R)-4\coth(I)\coth(R)\}\sin(I+R)$$
$$-\frac{1}{2}\lambda\sigma_0^3[\coth^2(I)-\coth^2(R)]\sin(I-R) \quad \text{on} \quad y=0 \tag{72}$$

In the above calculation, the approximation of $\sigma_I\fallingdotseq\sigma_R\fallingdotseq\sigma_0$ is employed, because the introduction of correction terms of σ_2 etc. into the term of σ_I or σ_R produces terms with a^4 or higher order terms while the present calculation is to the second power of a.

By the same reason, the wave numbers of k_I and k_R can be approximated with the first order value of k_A given by Eq. 57 as

$$k_I\fallingdotseq -k_R\fallingdotseq k_A \tag{73}$$

The above approximation should not be employed for the calculation of the phase

functions of $\sin(I\pm R)$ and $\cos(I\pm R)$ because a small difference in wave number may produce a reversal of phase angle at a large distance.

The velocity potential $\Phi_F^{(1)}$ is now obtained from Eq. 72 in a similar way with that for progressive waves. Then, the result is substituted into Eq. 69 to yield $\eta_F^{(1)}$. Finally the second order solution of bound waves with the approximation of Eq. 73 is obtained as

$$\left.\begin{aligned}\Phi_F^{(1)}&=\lambda\sigma_0\beta_{20}\sin(I+R)\\ \eta_F^{(1)}&=\lambda k_A b_{02}\cos(I-R),\end{aligned}\right\} \tag{74}$$

where:

$$\left.\begin{aligned}\beta_{20}&=-\frac{1}{4}(3+c^2)\\ b_{02}&=\frac{1}{2}(c+c^{-1})\\ c&=\coth k_A h.\end{aligned}\right\} \tag{75}$$

(3) Third order solution of bound waves

The third order surface conditions of Eqs. 4^3 and 5^3 are rewritten for $\Phi_F^{(2)}$ and $\eta_F^{(2)}$ by substituting Eqs. 61, 62 and 63 and by dropping the terms of progressive waves only and those of retrogressive waves only. The resultant equations contains the terms with λ and those with λ^2 while the terms of $\Phi_F^{(2)}$ and $\eta_F^{(2)}$ do not contain λ explicitly. Since the factor λ can take any value between 0 and 1, $\Phi_F^{(2)}$ and $\eta_F^{(2)}$ must be composed of the terms with λ and those with λ^2, and they can be treated separately. First, Eq. 4^3 becomes

$$\begin{aligned}\lambda:\ &\frac{1}{\lambda}\{g\eta_F^{(2)}(\lambda)+\Phi_{F_t}^{(2)}(\lambda)\}+\sigma_{RF}\Phi_{R_\tau}^{(0)}\\ &=-2\sigma_0\eta_I^{(1)}\Phi_{R_{\tau y}}^{(0)}-2\sigma_0\eta_R^{(0)}\Phi_{I_{\tau y}}^{(1)}-\frac{2}{\lambda}\sigma_0\eta_F^{(1)}\Phi_{I_{\tau y}}^{(0)}-\frac{2}{\lambda}\eta_I^{(0)}\Phi_{F_{ty}}^{(1)}\\ &\quad-2\sigma_0\eta_I^{(0)}\eta_R^{(0)}\Phi_{I_{\tau yy}}^{(0)}-\sigma_0\eta_I^{(0)2}\Phi_{R_{\tau yy}}^{(0)}\\ &\quad-2\eta_I^{(0)}\Phi_{I_x}^{(0)}\Phi_{R_{xy}}^{(0)}-2\eta_R^{(0)}\Phi_{I_x}^{(0)}\Phi_{I_{xy}}^{(0)}-2\eta_I^{(0)}\Phi_{R_x}^{(0)}\Phi_{I_{xy}}^{(0)}\\ &\quad-2\eta_I^{(0)}\Phi_{I_y}^{(0)}\Phi_{R_{yy}}^{(0)}-2\eta_R^{(0)}\Phi_{I_y}^{(0)}\Phi_{I_{yy}}^{(0)}-2\eta_I^{(0)}\Phi_{R_y}^{(0)}\Phi_{I_{yy}}^{(0)}\\ &\quad-2\Phi_{R_x}^{(0)}\Phi_{I_x}^{(1)}-2\Phi_{R_y}^{(0)}\Phi_{I_y}^{(1)}-\frac{2}{\lambda}\Phi_{I_x}^{(0)}\Phi_{F_x}^{(1)}-\frac{2}{\lambda}\Phi_{I_y}^{(0)}\Phi_{F_y}^{(1)}\qquad\text{on}\quad y=0,\end{aligned} \tag{76}$$

$$\begin{aligned}\lambda^2:\ &\frac{1}{\lambda^2}\{g\eta_F^{(2)}(\lambda^2)+\Phi_{F_t}^{(2)}(\lambda^2)+\sigma_{IF}\Phi_{I_\tau}^{(0)}\}\\ &=\{\text{same as the above except for the subscript}\\ &\quad I\text{ to be changed to }R\}\qquad\text{on}\quad y=0.\end{aligned} \tag{77}$$

Similarly, Eq. 5^3 is written as

$$\lambda:\ \frac{1}{\lambda}\{\Phi_{F_y}^{(2)}(\lambda)-\eta_{F_t}^{(2)}(\lambda)\}-\sigma_{RF}\eta_{R_\tau}^{(0)}=-2\eta_I^{(1)}\Phi_{R_{yy}}^{(0)}-2\eta_R^{(0)}\Phi_{I_{yy}}^{(0)}$$

$$-\frac{2}{\lambda}\eta_F^{(1)}\Phi_{I_{yy}}^{(0)}-\frac{2}{\lambda}\eta_I^{(0)}\Phi_{F_{yy}}^{(1)}-2\eta_I^{(0)}\eta_R^{(0)}\Phi_{I_{yyy}}^{(0)}-\eta_I^{(0)2}\Phi_{R_{yyy}}^{(0)}$$
$$+2\eta_{I_x}^{(1)}\Phi_{R_x}^{(0)}+2\eta_{R_x}^{(0)}\Phi_{I_x}^{(1)}+\frac{2}{\lambda}\eta_{F_x}^{(1)}\Phi_{I_x}^{(0)}+\frac{2}{\lambda}\eta_{I_x}^{(0)}\Phi_{F_x}^{(1)}$$
$$2\eta+{}^{(0)}_{I}\eta_{I_x}^{(0)}\Phi_{R_{xy}}^{(0)}+2\eta_R^{(0)}\eta_{I_x}^{(0)}\Phi_{I_{xy}}^{(0)}+2\eta_I^{(0)}\eta_{R_x}^{(0)}\Phi_{I_{xy}}^{(0)} \qquad \text{on} \quad y=0, \tag{78}$$

$$\lambda^2: \quad \frac{1}{\lambda^2}\{\Phi_{F_y}^{(2)}(\lambda^2)-\eta_{F_t}^{(2)}(\lambda^2)-\sigma_{IF}\eta_{I_z}^{(0)}\}$$
$$=\{\text{same as the above except for the subscript } I \text{ to be changed to } R\} \qquad \text{on} \quad y=0 \tag{79}$$

The calculation of these equations with the first and second order solutions given by Eqs. 22, 38 and 74 yields the following:

$$\frac{1}{\lambda}\{g\eta_F^{(2)}+\Phi_{F_t}^{(2)}\}-g\frac{\sigma_{RF}}{\sigma_0}\cos(R)=\frac{1}{2}k_A\sigma_0^2(4c+c^{-1})\cos(R)$$
$$+\frac{1}{4}k_A\sigma_0^2(3c^5+21c^3-11c)\cos(2I+R)$$
$$+\frac{1}{4}k_A\sigma_0^2(3c^5+9c^3-5+2c^{-1})\cos(2I-R) \qquad \text{on} \quad y=0, \tag{80}$$

$$\frac{1}{\lambda}\{g\Phi_{F_y}^{(2)}-g\eta_{F_t}^{(2)}\}+g\sigma_{RF}\sin(R)=-\frac{1}{2}k_A\sigma_0^3(c^3+2c)\sin(R)$$
$$-\frac{1}{4}k_A\sigma_0^3(c^3-2c)\sin(2I+R)-\frac{9}{4}k_A\sigma_0^3c^3\sin(2I-R)$$
$$\text{on} \quad y=0, \tag{81}$$

where:

$$\left.\begin{aligned}&(R)=(k_Rx-\sigma_Rt)\\&(2I\pm R)=(2k_I\pm k_R)x-(2\sigma_I\pm\sigma_R)t.\end{aligned}\right\} \tag{82}$$

In the above calculation, the approximation of $\sigma_I\fallingdotseq\sigma_R\fallingdotseq\sigma_0$ as well as of Eq. 73 is employed. The equations for λ^2 terms are omitted, since they can be written down without difficulty. Thus the equation for $\Phi_F^{(2)}(\lambda)$ is obtained as

$$\frac{1}{\lambda}\{g\Phi_{F_y}^{(2)}+\Phi_{F_{tt}}^{(2)}\}=-\left[2g\sigma_{RF}+\frac{1}{2}k_A\sigma_0^3(c^3+6c+c^{-1})\right]\sin(R)$$
$$+\frac{1}{4}k_A\sigma_0^3(9c^5+62c^3-31c)\sin(2I+R)$$
$$+\frac{1}{4}k_A\sigma_0^3(3c^5-5c+2c^{-1})\sin(2I-R) \tag{83}$$

The frequency corretion terms of σ_{RF} and σ_{IF} are determined from the periodicity condition as

$$\left.\begin{aligned}&\sigma_{RF}=-k_A^2\sigma_0C_2,\\&\sigma_{IF}=-\lambda^2k_A^2\sigma_0C_2,\\&\text{where:}\quad C_2=\frac{1}{4}(c^2+6+c^{-2}).\end{aligned}\right\} \tag{84}$$

The velocity potential $\Phi_F^{(2)}$ and the surface elevation $\eta_F^{(2)}$ are then solved from Eqs. 83 and 80 in a similar way with that for progressive waves as

$$\left.\begin{aligned}\Phi_F^{(2)}&=k_A\sigma_0\beta_{31}[\lambda\sin(2I+R)+\lambda^2\sin(2R+I)]\cosh k_A(y+h)\\&\quad+k_A\sigma_0\beta_{13}[\lambda\sin(2I-R)+\lambda^2\sin(2R-I)]\cosh 3k_A(y+h)\\\eta_F^{(2)}&=k_A^2 b_1[\lambda\cos(R)+\lambda^2\cos(I)]+k_A^2 b_{31}[\lambda\cos(2I+R)\\&\quad+\lambda^2\cos(2R+I)]+k_A^2 b_{13}[\lambda\cos(2I-R)+\lambda^2\cos(2R-I)],\end{aligned}\right\}\tag{85}$$

where:

$$\left.\begin{aligned}\beta_{31}&=-\frac{1}{32\cosh kh}(9c^5+62c^3-31c)\\\beta_{13}&=\frac{1}{32\cosh 3kh}(1+3c^{-2})(3c^5-5c+2c^{-1})\\b_1&=\frac{1}{4}(-c^2+2+c^{-2})\\b_{31}&=\frac{1}{32}(-3c^4-18c^2+5)\\b_{13}&=\frac{3}{32}(9c^4+27c^2-15+c^{-2}+2c^{-4}).\end{aligned}\right\}\tag{86}$$

(4) Correction of wave number

So far the correction to the angular frequency instead of the wave number has been considered. This frequency correction can be converted to the wave number correction under the condition of constant wave frequency. First, Eq. 63 is rewritten with the results of Eqs. 51 and 86 as

$$\left.\begin{aligned}\sigma_I&=\sigma_0\left[1+\frac{1}{2}(k_A a)^2(C_1-\lambda^2 C_2)\right]\\\sigma_R&=\sigma_0\left[1+\frac{1}{2}(k_A a)^2(\lambda^2 C_1-C_2)\right],\end{aligned}\right\}\tag{87}$$

where C_1 and C_2 are given by Eqs. 52 and 84.

Since the first order frequency of σ_0 is related to the wave number of finite amplitude waves through Eq. 17, the above equation is rewritten as

$$\left.\begin{aligned}\sigma_I^2&=g k_I\tanh k_I h\left[1+\frac{1}{2}(k_A a)^2(C_1-\lambda^2 C_2)\right]^2\\\sigma_R^2&=g k_R\tanh k_R h\left[1+\frac{1}{2}(k_A a)^2(\lambda^2 C_1-C_2)\right]^2.\end{aligned}\right\}\tag{88}$$

The first order approximation to wave number k_A is the same for both the progressive and retrogressive waves, and is given by

$$\sigma_I^2=\sigma_R^2=g k_A\tanh k_A h.\tag{89}$$

As in the derivation of Eq. 59 for progressive waves, the wave numbers k_I and k_R are related to k_A to the third order approximation as

$$\left.\begin{aligned} k_I &= k_A\left[1-\frac{1}{2}(k_A a)^2(K_1-\lambda^2 K_2)\right] \\ k_R &= -k_A\left[1-\frac{1}{2}(k_A a)^2(\lambda^2 K_1-K_2)\right], \end{aligned}\right\} \tag{90}$$

where:

$$K_2=\frac{2C_2}{1+k_A h(\coth k_A h-\tanh k_A h)}. \tag{91}$$

The above equation predicts the increase in wave number or the shortening of wavelength for both the progressive and retrogressive waves as a result of the interaction between them. Such change in wave number has been calculated for two trains of deep water waves by Longuet-Higgins and Phillips[12]. Their prediction for the phase velocity change for the case of two opposing wave trains with the same frequency is in agreement with the present calculation.

2.3 Standing Waves

When the amplitudes of progressive and retrogressive waves are equal as in the case of perfect reflection, the factor λ becomes 1 and the expressions for Φ, η, and σ are simplified as follows:

$$\left.\begin{aligned} \frac{k^2}{\sigma_0}\Phi=&\{2\beta_0+2\varepsilon^2\alpha_{01}\sigma t-2\varepsilon\beta_{11}\sin\sigma t\cos kx\cosh k(y+h) \\ &-2\varepsilon^2\beta_{22}\sin 2\sigma t\cos 2kx\cosh 2k(y+h) \\ &-\varepsilon^3\beta_{33}\sin 3\sigma t\cos 3kx\cosh 3k(y+h)\} \\ &-\{\varepsilon^2\beta_{20}\sin 2\sigma t+\varepsilon^3\beta_{31}\sin 3\sigma t\cos kx\cosh k(y+h) \\ &+\varepsilon^3\beta_{13}\sin\sigma t\cos 3kx\cosh 3k(y+h)\} \\ k\eta=&\{(2\varepsilon+\varepsilon^3 b_{11})\cos\sigma t\cos kx+2\varepsilon^2 b_{22}\cos 2\sigma t\cos 2kx \\ &+\varepsilon^3 b_{33}\cos 3\sigma t\cos 3kx\}+\{\varepsilon^2 b_{02}\cos 2kx \\ &+\varepsilon^3 b_1\cos\sigma t\cos kx+\varepsilon^3 b_{31}\cos 3\sigma t\cos kx \\ &+\varepsilon^3 b_{13}\cos\sigma t\cos 3kx\} \\ \sigma=&\sigma_0\left[1+\frac{1}{2}\varepsilon^2(C_1-C_2)\right] \end{aligned}\right\} \tag{92}$$

with $\varepsilon=ka$.

Here the wave number k is that of finite amplitude standing waves, common to the incident and reflected waves; the approximation of Eq. 73 has not been employed.

These results are in complete agreement with those by Tadjbaksh and Keller[10] if the first order amplitude of incident wave a is rewritten with that of standing waves as $a'=2a$. In the present forms of representation, the effect of wave interference is clearly identified as the terms inside the second braces for Φ and η, and as C_2 for σ. These interference terms cause a shortening of wavelength and increase of standing wave height more than twice the incident wave height.

First, the change in wavelength is calculated from Eq. 90 by taking the tems of ε up to the second power. This is given by

$$\frac{L_S}{L_A}=1+\frac{1}{2}\varepsilon^2[K_1-K_2]. \tag{93}$$

While the wavelength of progressive waves increases from the first order approximation of L_A by the rate of $\frac{1}{2}\varepsilon^2 K_1$ as the wave amplitude increases, the wavelength of standing waves L_S decreases from that of progressive waves by the rate of $\frac{1}{2}\varepsilon^2 K_2$. As seen in Fig. 1, the value of K_2 exceeds that of K_1 in the range of h/L greater than about 0.17; in this range L_S is shorter than L_A. This shortening of wavelength due to wave interaction becomes less conspicuous as the water becomes shallow relative to wavelength, because the value of K_1 increases more rapidly than that of K_2 at shallow water. The above phenomenon has been predicted by Tadjbaksh and Keller although they did not identify the wave interaction term of K_2. Later Fultz[13] experimentally verified the decrease of angular frequency for a fixed wavelength in the relative depth of $h/L>0.14$ and the increase of angular frequency for $h/L<0.14$; the difference in the critical value of h/L for the reversal of frequency change is possibly due to the effect

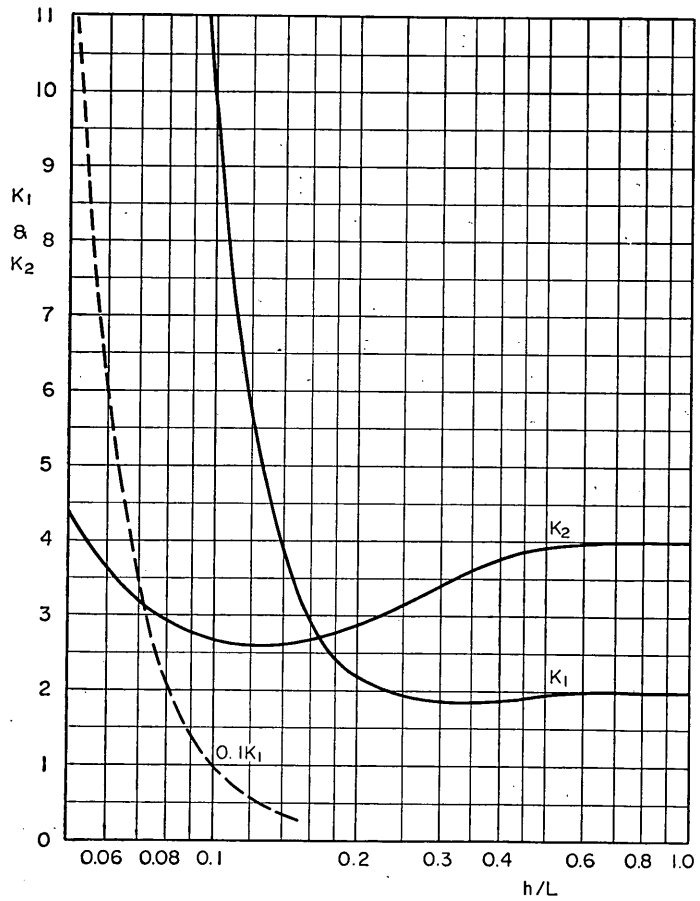

Fig. 1 Wavelength Coefficients, K_1 and K_2

of higher order terms more than the fifth which have been ignored in the theory.

Next, the height of standing waves denoted with H_S is calculated from Eq. 92 for $x=0$ as

$$H_S=4a\left[1+\frac{1}{2}\varepsilon^2(b_{11}+b_{33})+\frac{1}{2}\varepsilon^2(b_1+b_{31}+b_{13})\right]. \tag{94}$$

Since the height of incident waves denoted with H_I is given by Eq. 55, the standing wave height is expressed with respect to H_I as

$$\frac{H_S}{2H_I}=1+\frac{\frac{1}{2}\varepsilon^2(b_1+b_{31}+b_{13})}{1+\frac{1}{2}\varepsilon^2(b_{11}+b_{33})}. \tag{95}$$

The calculation of the coefficients b_1, b_{31} and b_{13} by Eq. 87 shows that the sum of these coefficients, $(b_1+b_{31}+b_{13})$, is always positive; hence the standing wave height is greater than twice the incident wave height. The increase of H_S over $2H_I$ is estimated as about 10 to 15% at most. For the accurate estimation of $H_S/2H_I$, the development of higher order theory of wave interaction is necessary because the accuracy of the present third order approximation is only enough to predict the increase of H_S over $2H_I$ qualitatively.

3. Apparent Coefficient of Wave Reflection

3.1 Discussion of Healy's Method

Now let us consider the technique in measurement of reflection coefficient. The most commonly used method is that of Healy, which was mentioned in Chapter 1. This method is justified for waves of infinitely small amplitudes as shown in the following.

By taking the first order terms of surface displacement, we have the following expressions for incident and reflected waves:

$$\left.\begin{aligned}\eta_I&=a\cos(kx-\sigma t)\\ \eta_R&=\lambda a\cos(kx+\sigma t).\end{aligned}\right\} \tag{96}$$

The resultant surface displacement of partial standing waves is then given as

$$\eta=\eta_I+\eta_R=(1+\lambda)a\cos kx\cos\sigma t+(1-\lambda)a\sin kx\sin\sigma t \tag{97}$$

The above expressions is rewritten by means of the trigonometric identity as

$$\eta=a\sqrt{1+2\lambda\cos 2kx+\lambda^2}\cos(\sigma t-\theta), \tag{98}$$

where:

$$\theta=\tan^{-1}\left[\frac{(1-\lambda)\sin kx}{(1+\lambda)\cos kx}\right]. \tag{99}$$

The amplitude of partial standing waves, therefore, varies with respect to x. The maximum and minimum wave heights appear at the following positions with the values of

$$\left.\begin{aligned} &H_{\max}=2a(1+\lambda) \quad \text{at} \quad kx=n\pi \quad \text{or} \quad x=nL/2 \\ &H_{\min}=2a(1-\lambda) \quad \text{at} \quad kx=(2n+1)\pi/2 \quad \text{or} \quad x=(2n+1)L/4 \\ &\qquad\qquad\qquad\qquad\qquad\qquad\qquad\qquad \text{with} \quad n=0,\ 1,\ 2,\cdots \end{aligned}\right\} \tag{100}$$

Since the incident wave height H_I is $2a$ and the reflected wave height is $2\lambda a$ in the first order approximation, they are recovered from the maximum and minimum wave heights shown in the above as

$$\left.\begin{aligned} H'_I&=\frac{1}{2}(H_{\max}+H_{\min}) \\ H'_R&=\frac{1}{2}(H_{\max}-H_{\min}), \end{aligned}\right\} \tag{101}$$

which is the same with Eq. 1. The dashes for incident and reflected heights are attached here in order to identify them as the values calculated with the maximum and minimum wave heights. The reflection coefficient is then calculated as

$$K'_R=\frac{H'_R}{H'_I}=\frac{H_{\max}-H_{\min}}{H_{\max}+H_{\min}}. \tag{102}$$

The above formulae are convenient ones for wave experiments. As long as the periodic variation of wave height with a distance of $L/2$ is observed in a wave channel, the heights of incident and reflected waves, and the value of reflection coefficient are easily calculated. The assumption of infinitely small amplitude, or the employment of first order terms only, however, causes some errors in the values of these. As a preliminary calculation, let us employ the theory of second order approximation. Since the wave number does not change with respect to ε to this order of approximation, the surface displacement is given by

$$\begin{aligned} \frac{\eta}{a}=&\lambda\varepsilon b_{02}\cos 2kx+\cos(kx-\sigma t)+\lambda\cos(kx+\sigma t) \\ &+\varepsilon b_{22}[\cos 2(kx-\sigma t)+\lambda^2\cos 2(kx+\sigma t)]. \end{aligned} \tag{103}$$

The surface displacement at $x=0$ is

$$\left.\frac{\eta}{a}\right|_{x=0}=\lambda\varepsilon b_{02}+(1+\lambda)\cos\sigma t+\varepsilon b_{22}(1+\lambda^2)\cos 2\sigma t \tag{104}$$

Unless the amplitude of the second harmonic become large to such an extent as to produce a secondary crest at $t=\pi/\sigma$, the wave height at this position is given by the following

$$H_{\max}=(1+\lambda)a \quad \text{for} \quad (1+\lambda)>4\varepsilon b_{22}(1+\lambda^2) \tag{105}$$

The surface displacement at the nodal point of $x=\pi/2k$ is expressed as

$$\left.\frac{\eta}{a}\right|_{x=\pi/2k}=-\lambda\varepsilon b_{02}+(1-\lambda)\cos\sigma t+\varepsilon b_{22}(1+\lambda^2)\cos 2\sigma t \tag{106}$$

Depending upon the value of λ as well as those of ε and b_{22}, the relative ampli-

tude of the second harmonic to the first harmonic can become large enough to produce a secondary crest at $t=\pi/\sigma$. For example, the first harmonic of $\cos\sigma t$ vanishes for the case of $\lambda=1$, leaving the second harmonic only. Since the first order theory gives $\eta=0$ at $x=\pi/2k$, the presence of second harmonic represents a finite amplitude effect. As will be understood from the development of the theory, this second harmonic is inherent to the original profiles of incident and reflected waves.

Equation 106 is differentiated with respect to t and set to zero in order to find the time at which the surface displacement becomes the highest or the lowest; thus,

$$\frac{d\eta}{dt}=-a\sigma[(1-\lambda)+4\varepsilon b_{22}(1+\lambda^2)\cos\sigma t]\sin\sigma t\equiv 0. \tag{107}$$

The solution of the above equation for $0\leq t\leq\pi/\sigma$ is

$$\left.\begin{aligned} &t_1=0\\ &t_2=\frac{1}{\sigma}\cos^{-1}\left[\frac{-(1-\lambda)}{4\varepsilon b_{22}(1+\lambda^2)}\right] \quad \text{if} \quad (1-\lambda)<4\varepsilon b_{22}(1+\lambda^2)\\ &t_3=\pi/\sigma. \end{aligned}\right\} \tag{108}$$

If the solution of $t=t_2$ exists, this gives the minimum value of η; if not, $t=t_3$ gives $\eta_{\min}$. Thus the wave height at $x=\pi/2k$ is obtained as

$$\left.\begin{aligned} H_{\min}&=2(1-\lambda)a \qquad \text{for} \quad (1-\lambda)\geq 4\varepsilon b_{22}(1+\lambda^2)\\ H_{\min}&=2(1-\lambda)a+\Delta H \qquad \text{for} \quad (1-\lambda)<4\varepsilon b_{22}(1+\lambda^2) \end{aligned}\right\} \tag{109}$$

where:

$$\Delta H=\frac{a}{8\varepsilon b_{22}(1+\lambda^2)}[4\varepsilon b_{22}(1+\lambda^2)-(1-\lambda)]^2. \tag{110}$$

The maximum height of Eq. 105 and the minimum height of Eq. 109 are now substituted into Eq. 102 for the calculation of the reflection coefficient. The result is,

$$\left.\begin{aligned} K'_R&=\lambda \qquad \text{for} \quad (1-\lambda)\geq 4\varepsilon b_{22}(1+\lambda^2)\\ K'_R&=\frac{\lambda-\Delta H/4a}{1+\Delta H/4a} \qquad \text{for} \quad (1-\lambda)<4\varepsilon b_{22}(1+\lambda^2). \end{aligned}\right\} \tag{111}$$

When the first equation of the above is applied, the reflection coefficient by Eq. 102 agrees with the amplitude ratio of reflected waves to incident waves. When the second equation of the above is applied, however, the reflection coefficient by Eq. 102 is smaller than the amplitude ratio because of the presence of the term of $\Delta H/4a$; the application of Eq. 102 to such a condition causes an underestimation of reflection coefficient.

3.2 Calculation of Apparent Reflection Coefficient

The surface displacement of partial standing waves to the third order approximation is given by the following equation:

$$\frac{\eta}{a}=\lambda\varepsilon b_{02}\cos(k_I-k_R)x+\{\cos(k_Ix-\sigma t)+\lambda\cos(k_Rx-\sigma t)\}$$
$$+\varepsilon b_{22}\{\cos 2(k_Ix-\sigma t)+\lambda^2\cos 2(k_Rx-\sigma t)\}$$
$$+\frac{1}{2}\varepsilon^2 b_{11}\{\cos(k_Ix-\sigma t)+\lambda^3\cos(k_Rx-\sigma t)\}$$
$$+\frac{1}{2}\varepsilon^2 b_{33}\{\cos 3(k_Ix-\sigma t)+\lambda^3\cos 3(k_Rx-\sigma t)\}$$
$$+\frac{1}{2}\lambda\varepsilon^2 b_1\{\lambda\cos(k_Ix-\sigma t)+\cos(k_Rx-\sigma t)\}$$
$$+\frac{1}{2}\lambda\varepsilon^2 b_{31}\{\cos[(2k_I+k_R)x-3\sigma t]+\lambda\cos[(2k_R+k_I)x-3\sigma t]\}$$
$$+\frac{1}{2}\lambda\varepsilon^2 b_{13}\{\cos[(2k_I-k_R)x-\sigma t]+\lambda\cos[(2k_R-k_I)x-\sigma t]\}. \tag{112}$$

Since the wave numbers of incident and reflected waves are slightly different as expressed in Eq. 90, the average of $|k_I|$ and $|k_R|$ is defined here as

$$\bar{k}=\frac{1}{2}(|k_I|+|k_R|)=k_A\left[1-\frac{1}{4}\varepsilon^2(1+\lambda^2)(K_1-K_2)\right]. \tag{113}$$

With this average wave number, k_I and k_R are rewritten as

$$\left.\begin{aligned}k_I&=\bar{k}+\Delta_k\\ k_R&=-\bar{k}+\Delta_k,\end{aligned}\right\} \tag{114}$$

where:

$$\Delta_k=\frac{1}{4}\varepsilon^2(1-\lambda^2)(K_1+K_2). \tag{115}$$

The surface displacement is then expressed with $\bar{k}$ and Δ_k as

$$\frac{\eta}{a}=\varepsilon b_{02}\cos 2\bar{k}x+[\cos(\bar{k}x-\sigma t')+\lambda\cos(\bar{k}x+\sigma t')]$$
$$+\varepsilon b_{22}[\cos 2(\bar{k}x-\sigma t')+\lambda^2\cos 2(\bar{k}x+\sigma t')]$$
$$+\frac{1}{2}\varepsilon^2 b_{33}[\cos 3(\bar{k}x-\sigma t')+\lambda^3\cos 3(\bar{k}x+\sigma t')]$$
$$+\frac{1}{2}\varepsilon^2 b_{11}[\cos(\bar{k}x-\sigma t')+\lambda^3\cos(\bar{k}x+\sigma t')]$$
$$+\frac{1}{2}\lambda\varepsilon^2 b_1[\lambda\cos(\bar{k}x-\sigma t')+\cos(\bar{k}x+\sigma t')]$$
$$+\frac{1}{2}\lambda\varepsilon^2 b_{31}[\cos(\bar{k}x-3\sigma t'-2\Delta_k x)+\lambda\cos(\bar{k}x+3\sigma t'+2\Delta_k x)]$$
$$+\frac{1}{2}\lambda\varepsilon^2 b_{13}[\cos(3\bar{k}x-\sigma t'+2\Delta_k x)+\lambda\cos(3\bar{k}x+\sigma t'-2\Delta_k x)], \tag{116}$$

where:

$$\sigma t' = \sigma t - \Delta_k x. \tag{117}$$

The calculation of wave height at arbitrary location from the above equation cannot be made in explicit form; it is possible only numerically or at special locations. Several runs of numerical computation, however, have shown that the maximum wave heights appear at $\bar{k}x \fallingdotseq n\pi$ and the minimum heights at $\bar{k}x \fallingdotseq (2n+1)\pi/2$ as in the case of small amplitnde waves. The term of $2\Delta_k x$ in the third order interaction causes some variation in wave heights at nodes and anti-nodes. But the amount of this variation is rather insignificant, and can be ignored unless the distance from the source of wave reflection is large. Therefore, the wave height at $kx=0$ is taken as $H_{\max}$ and the height at $\bar{k}x=\pi/2$ as $H_{\min}$ for the calculation of apparent reflection coefficient in Eq. 102.

From Eq. 116 the surface displacement at $x=0$ is obtained as

$$\left.\frac{\eta}{a}\right|_{x=0} = \varepsilon b_{02} + \left[(1+\lambda) + \frac{1}{2}\varepsilon^2(1+\lambda^3)b_{11} + \frac{1}{2}\varepsilon^2\lambda(1+\lambda)(b_1+b_{13})\right]\cos\sigma t$$
$$+\varepsilon b_{22}(1+\lambda^2)\cos 2\sigma t + \frac{1}{2}\varepsilon^2[(1+\lambda^3)b_{33} + \lambda(1+\lambda)b_{31}]\cos 3\sigma t. \tag{118}$$

Since the amplitude of the twice frequency oscillation in the above is not large, the wave height at $x=0$ is calculated as

$$\frac{H_{\max}}{a} = 2(1+\lambda) + \varepsilon^2(1+\lambda^3)(b_{11}+b_{33}) + \varepsilon^2\lambda(1+\lambda)(b_1+b_{13}+b_{31}). \tag{119}$$

The first and second terms represent the sum of incident and reflected wave heights. The third term represents the wave interaction effect. As in the discussion of Eq. (95), this term is always positive; hence $H_{\max}$ is greater than the sum of incident and reflected wave heights.

The surface displacement at $kx=\pi/2$ is obtained as in the following by ignoring the term of $2\Delta_k x$:

$$\left.\frac{\eta}{a}\right|_{x=\pi/2k} = A\sin\sigma t - B\cos 2\sigma t - C\sin 3\sigma t, \tag{120}$$

where:

$$\left.\begin{aligned} A &= (1-\lambda) + \frac{1}{2}\varepsilon^2[(1-\lambda^3)b_{11} - \lambda(1-\lambda)(b_1+b_{13})] \\ B &= \varepsilon(1+\lambda^2)b_{22} \\ C &= \frac{1}{2}\varepsilon^2[(1-\lambda^3)b_{33} - \lambda(1-\lambda)b_{31}]. \end{aligned}\right\} \tag{121}$$

At this location, the amplitude of the twice frequency oscillation can become large enough to produce secondary crest at wave trough; in such a case, the lowest surface elevation occurrs between $t=\pi/\sigma$ and $3\pi/2\sigma$. The examination of secondary crest appearance is made by taking the derivative of Eq. 120 with respect to t and by searching the time of $\eta_{\min}$ as in the derivation of Eq. 108. By this procedure the minimum wave height is obtained as

$$\frac{H_{\min}}{a} = 2(A+C) \qquad \text{if} \quad \eta=\eta_{\min} \quad \text{at} \quad t=3\pi/2\sigma \tag{122.1}$$

$$\frac{H_{\min}}{a}=A+2B+C+2[B+4C\sin\sigma t_1]\sin^2\sigma t_1$$

$$\text{if}\quad \eta=\eta_{\min}\quad \text{at}\quad t=t_1, \tag{122.2}$$

where:

$$\sin\sigma t_1=(-B+\sqrt{B^2+9C^2-3AC})/6C. \tag{123}$$

Equation 122.1 is applied under the following condition:

$$\left.\begin{aligned} &B^2+9C^2-3AC<0 \\ &\text{or} \\ &B^2+9C^2-3AC>0,\quad A-4B+9C>0, \\ &\qquad\text{and}\quad \begin{cases} B-6C>0, \\ \text{or} \\ B-6C<0\quad\text{and}\quad \eta(3\pi/2\sigma)<\eta(t_1). \end{cases} \end{aligned}\right\} \tag{124}$$

When one of the above conditions is satisfied, the apparent heights of incident and reflected waves are calculated as

$$\left.\begin{aligned} H_I'&=2a\left[1+\frac{1}{2}\varepsilon^2(b_{11}+b_{33})+\frac{1}{2}\varepsilon^2\lambda^2(b_1+b_{13}+b_{31})\right] \\ H_R'&=2\lambda a\left[1+\frac{1}{2}\lambda^2\varepsilon^2(b_{11}+b_{33})+\frac{1}{2}\varepsilon^2(b_1+b_{13}+b_{31})\right]. \end{aligned}\right\} \tag{125}$$

The third terms in the brackets of the above equations represent the effect of wave interaction, by which the apparent reflection coefficient may increase by up to 20% from the true value. This increase occurrs for a small value of reflection coefficient, however. Hence the increase of apparent reflection coefficient

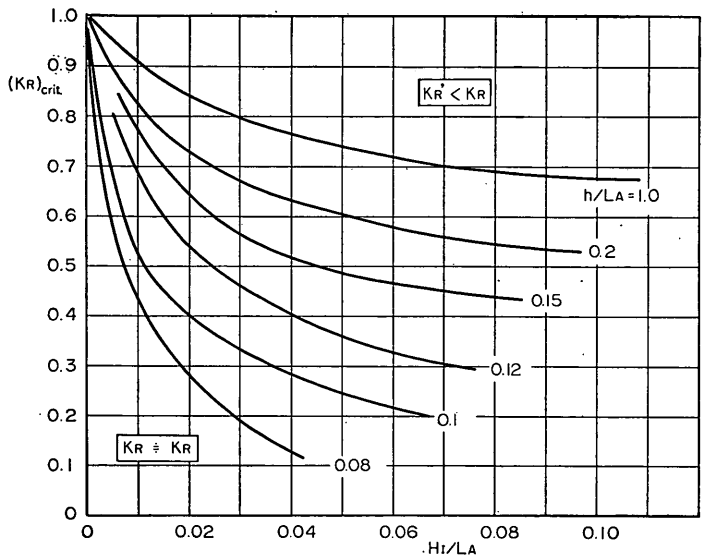

Fig. 2 Critical Reflection Coefficient for Finite Amplitude Effect

in the absolute value is not large.

When the condition of Eq. 124 is not satisfied, the minimum wave height is given by Eq. 122.2; the value of $H_{\min}$ is larger than $2(A+C)$. In this case, the apparent incident wave height is larger than that given by Eq. 125 and the apparent reflected wave height becomes smaller than that given by Eq. 125. This causes the apparent decrease of reflection coefficient. For a structure of high reflectivety at the relatively shallow water, K'_R may become smaller than $K_R/2$. The region in which K'_R is smaller than K_R is approximately shown in Fig. 2, which has been determined by numerical analysis. For the data below

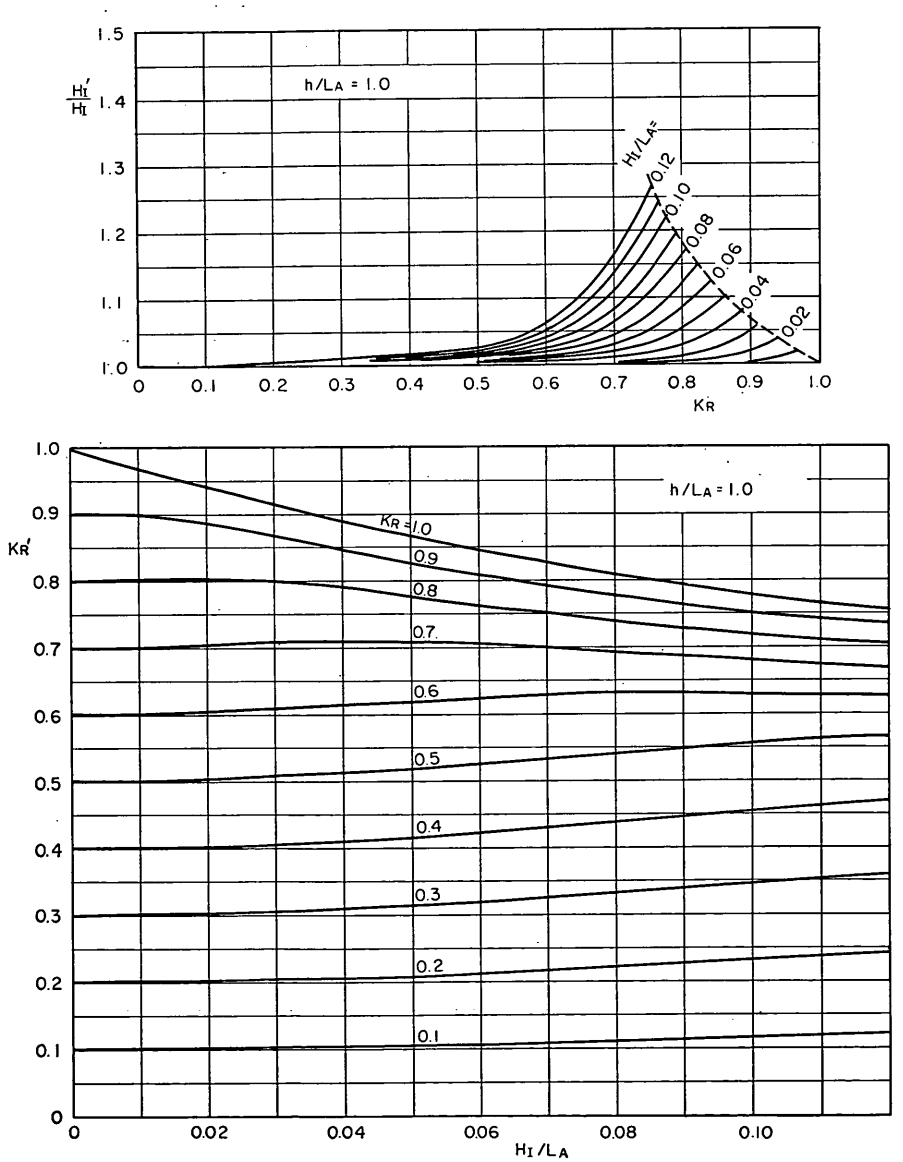

Fig. 3 Apparent Reflection Coefficient and Incident Wave Height for $h/L_A=1.0$

the curve corresponding to the specific value of h/L_A, the reflection coefficient determined by means of Eq. 102 will be a little larger than the true value, but the difference will not be large. For the data above the curve, some correction to the calculated value of reflection coefficient will be necessary in order to estimate the true value.

The incident wave height calculated by means of Eq. 101 also needs a correction, especially for the data in the region of $K'_R < K_R$. If the maximum wave height is approximated with

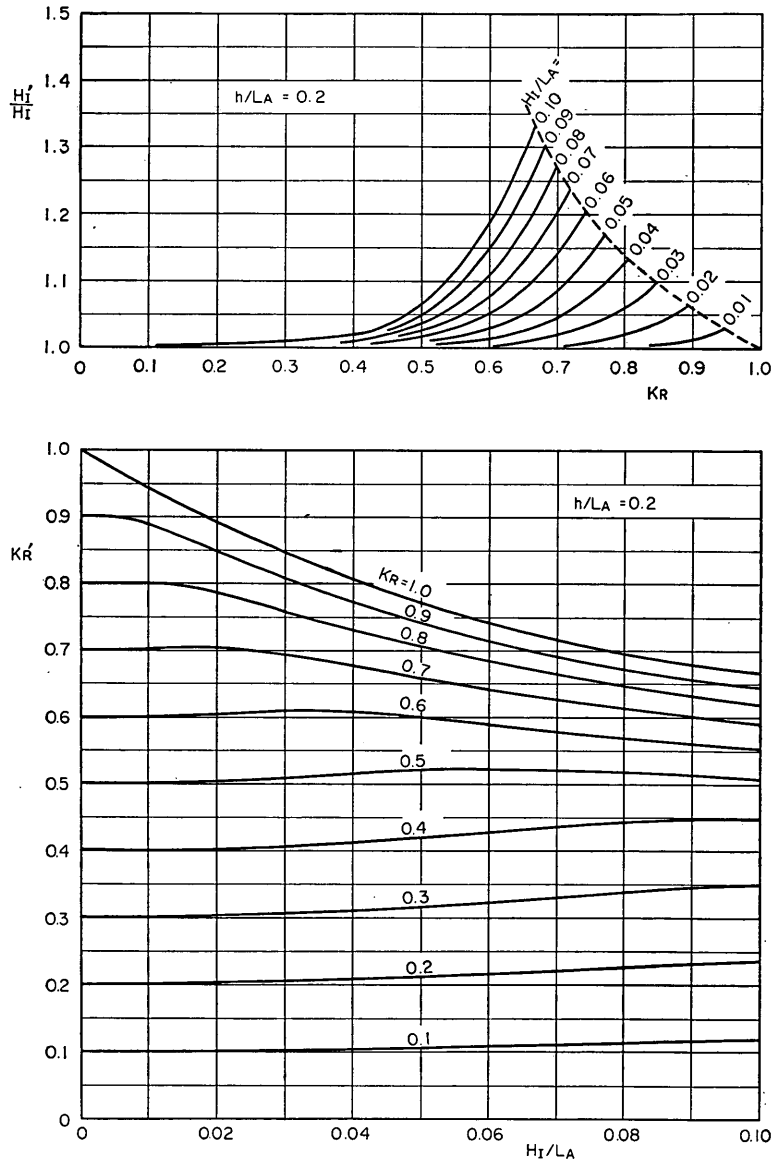

Fig. 4 Apparent Reflection Coefficient and Incident Wave Height for $h/L_A=0.2$

$$H'_{max}=(1+K_R)H_I \tag{126}$$

by ignoring the wave interference effect, then the apparent indident wave height can be related to the true height as

$$H'_I=\frac{1+K_R}{1+K'_R}H_I \tag{127}$$

The ratio of H'_I/H_I may become greater than 1.5 in certain cases.

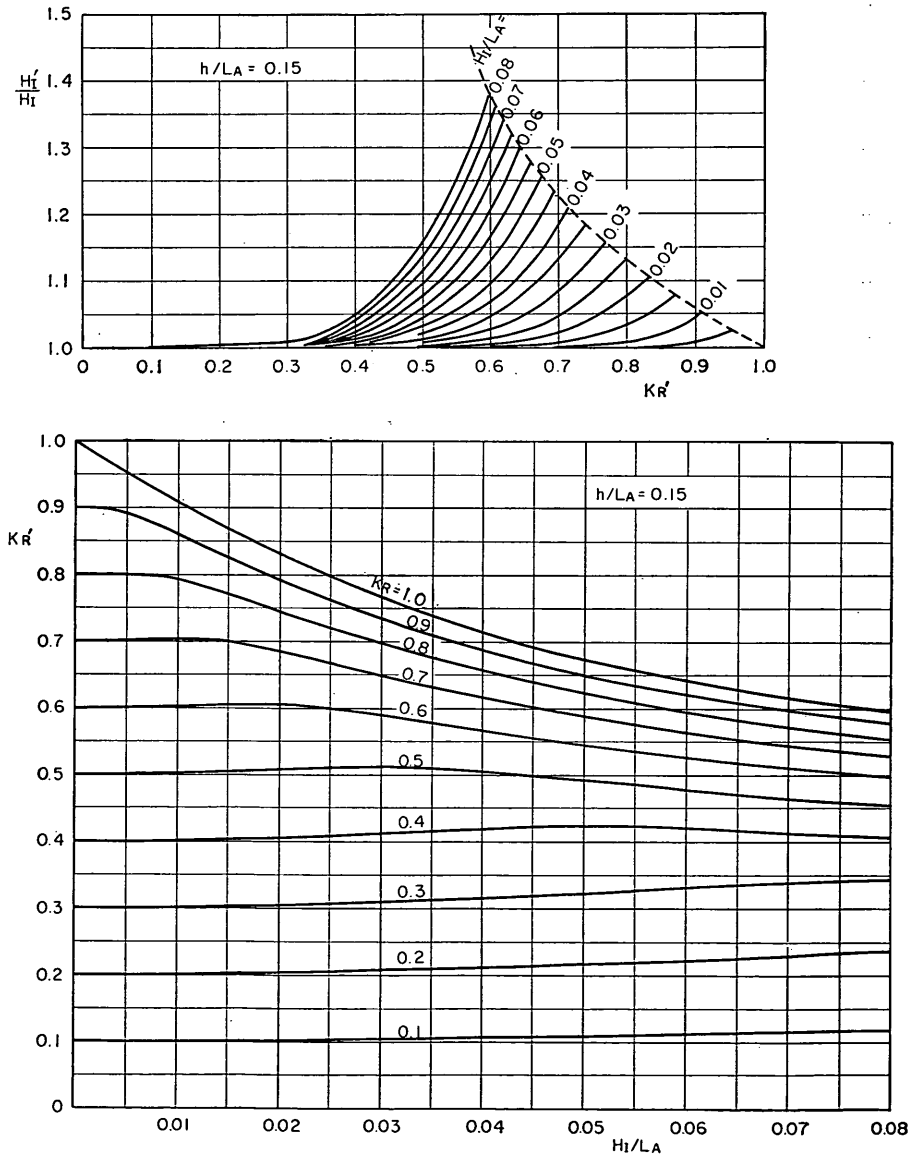

Fig. 5 Apparent Reflection Coefficient and Incident Wave Height for $h/L_A=0.15$

The calculation of K_R and H_I from the measured values of K'_R and H'_I is almost impossible even numerically, although the reverse is possible. Therefore, the apparent values of K'_R and H'_I have been computed for various values of K_R, H_I/L_A, and h/L_A and plotted in Figs. 3 through 8, which are prepared for the relative depth of h/L_A=1.0, 0.2, 0.15, 0.12, 0.10 and 0.08, respectively. The upper part of each figure shows the ratio of H'_I/H_I against the apparent reflection coefficient K'_R with the parameter of incident wave steepness H_I/L_A. With

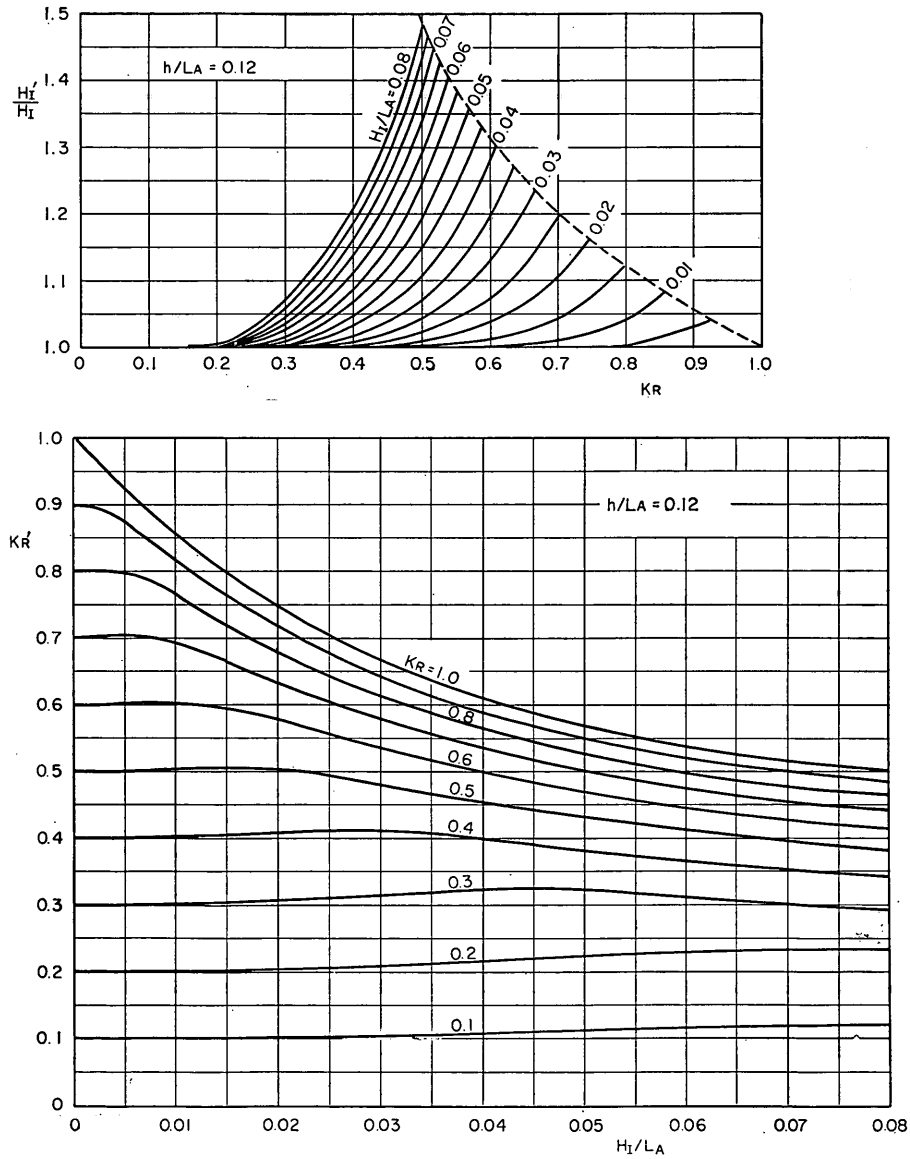

Fig. 6 Apparent Reflection Coefficient and Incident Wave Height for h/L_A=0.12

several repetitions of interpolation, the actual height of incident waves H_I will be estimated from the measured values of K'_R and H'_I. The actual value of reflection coefficient K_R will then be estimated from the lower part of the figure.

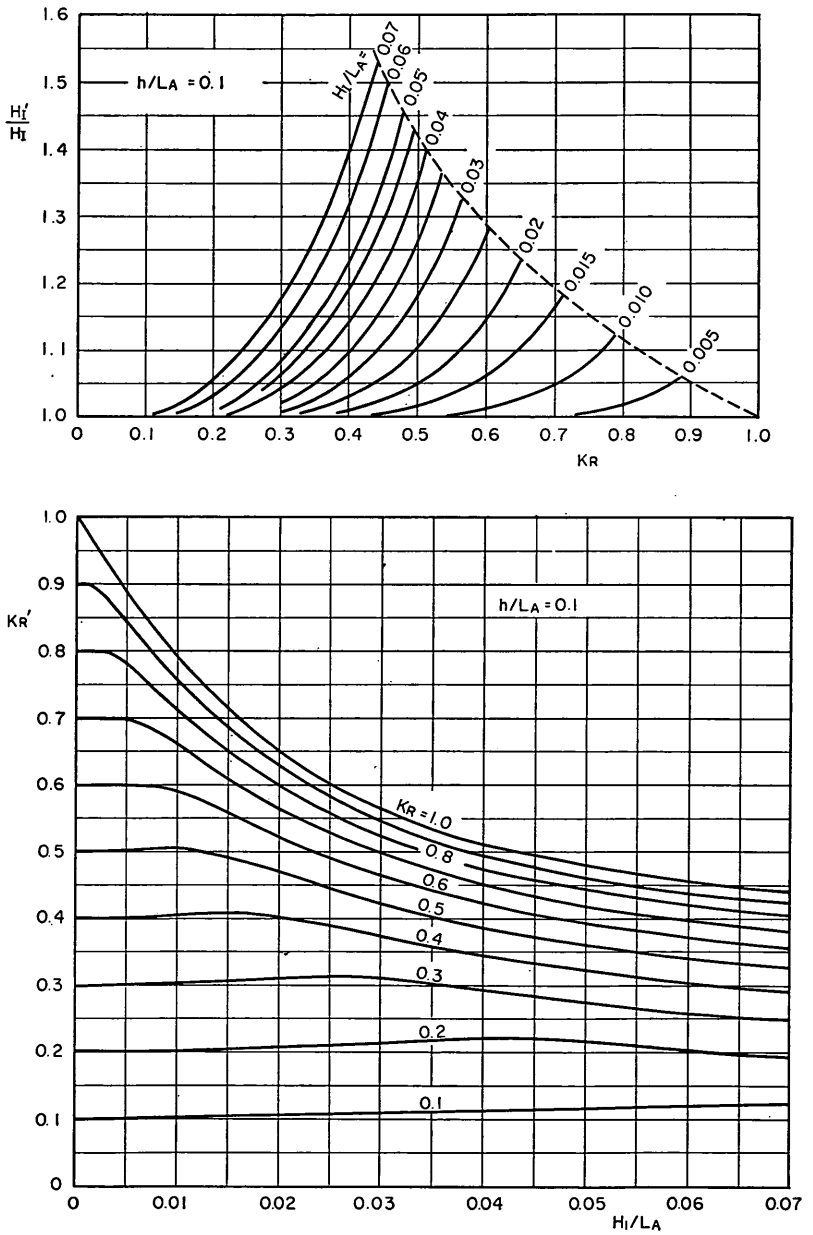

Fig. 7 Apparent Reflection Coefficient and Incident Wave Height for h/L_A=0.10

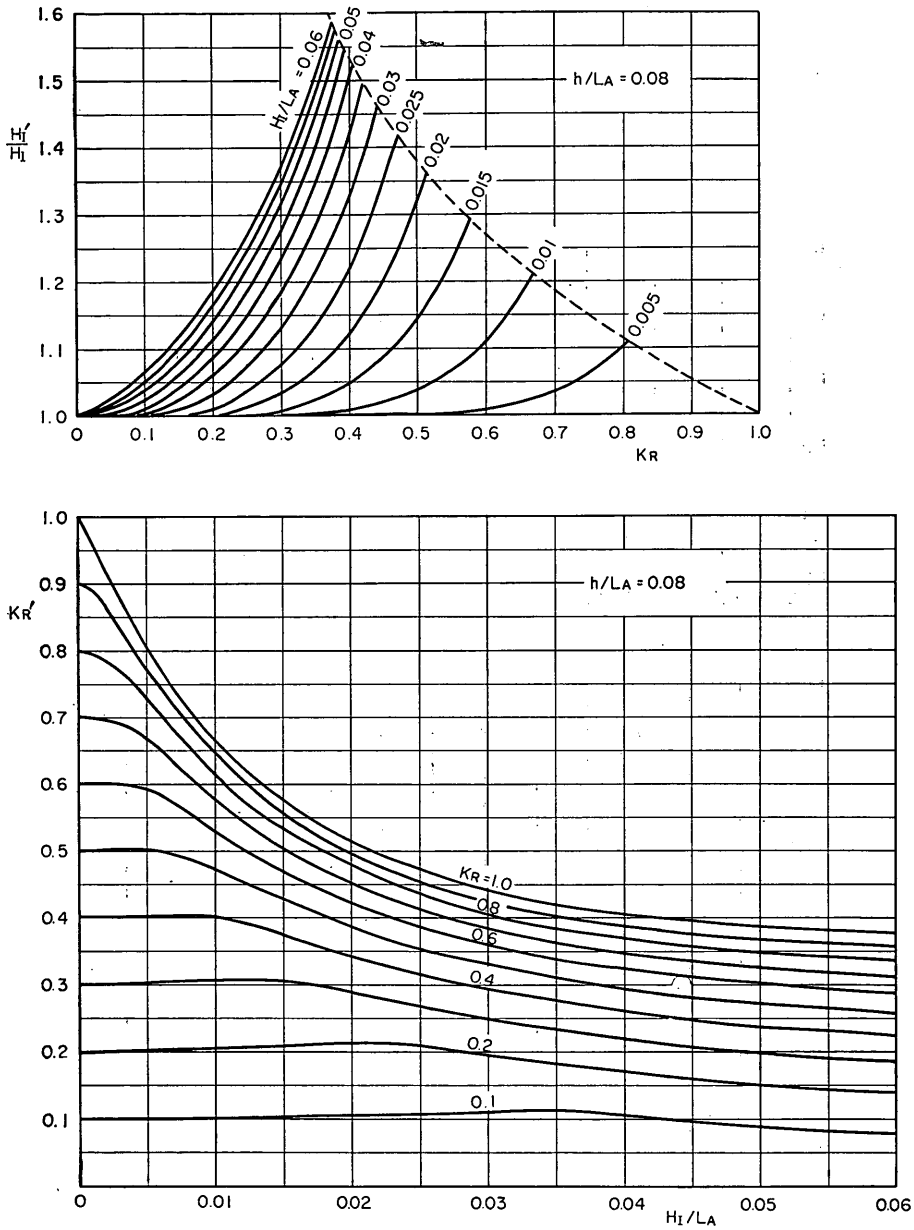

Fig. 8 Apparent Reflection Coefficient and Incident Wave Height for $h/L_A=0.08$

3.3 Apparent Coefficient of Perfect Reflection

The most significant effect of finite amplitudes on reflection coefficient is observed in the case of perfect reflection, in which the reflected wave height is equal to the incident wave height. Since $\lambda=1$ for perfect reflection, the wave numbers of k_I and k_R are equal to $\bar{k}$ and the surface displacement is given by

Eq. 92. At the nodal point of $x=\pi/2\bar{k}$, the surface displacement becomes

$$\left.\frac{\eta}{a}\right|_{x=2\pi/k} = -\varepsilon b_{02} - 2\varepsilon b_{22}\cos 2\sigma t, \tag{128}$$

showing the twice frequncy oscillation. The apparent coefficient of perfect wave reflection is calculated as in the following, since $H_{\max}$ is given by Eq. 94 and $H_{\min}$ by $4a\varepsilon b_{22}$:

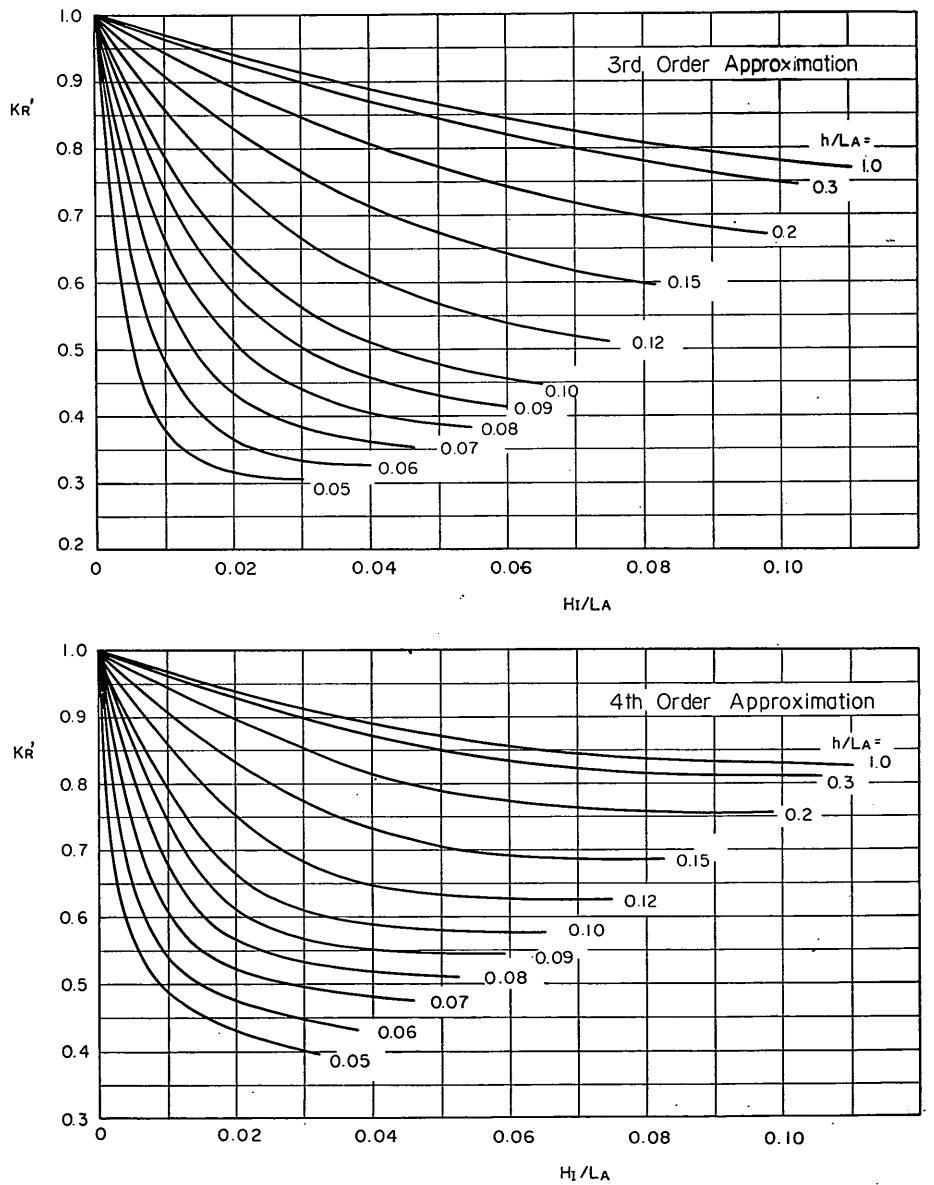

Fig. 9 Apparent Coefficient of Perfect Reflection

$$K'_R=1-\frac{2\varepsilon b_{22}}{1+\varepsilon b_{22}+\frac{1}{2}\varepsilon^2(b_{11}+b_{33}+b_1+b_{31}+b_{13})}. \tag{129}$$

As seen in the upper part of Fig. 9 which shows the variations of K'_R for various values of h/L_A and H_I/L_A, the decrease of K'_R from 1.0 is very large for waves of large steepness at relatively shallow water.

The apparent coefficient of perfect wave reflection can be calculated more accurately with the theory of standing waves of higher order approximation. According to the fourth order approximation[14], the surface displacement at $x=\pi/2k$ has the fourth harmonic component of oscillation as in the following:

$$\frac{\eta}{a}=\left[-\varepsilon b_{02}-\frac{1}{6}\varepsilon^3(b^*_{02}+b_{04})\right]+\left[-\varepsilon b_{22}+\frac{1}{6}\varepsilon^3(b^*_{22}+b_{24})\right]\cos 2\sigma t$$
$$+\frac{1}{6}\varepsilon^3(-b_{42}+b_{44})\cos 4\sigma t \tag{130}$$

where:

$$\left.\begin{aligned}
b^*_{02}&=\frac{1}{64}(-27c^5+288c^3+168c-210c^{-1}-45c^{-3}+18c^{-5})\\
b^*_{22}&=\frac{1}{64}(-81c^9-54c^7+423c^5-583c^3+108c-195c^{-1}-18c^{-3})\\
b_{42}&=\frac{1}{64(3+4c^{-2})}(-81c^7-1053c^5+63c^3-283c+282c^{-1})\\
b_{04}&=\frac{1}{64}(54c^7+243c^5+198c^3+6c-198c^{-1}+63c^{-3}+18c^{-5})\\
b_{24}&=\frac{1}{64(3+c^{-2})}(324c^7+2484c^5-1152c^3-2072c\\
&\qquad\qquad +1092c^{-1}+420c^{-3}-72c^{-5})\\
b_{44}&=\frac{1}{64(5+c^{-2})}405c^9+81c^7+522c^5-262c^3+c+21c^{-1})
\end{aligned}\right\} \tag{131}$$

The fourth order terms of $(b^*_{22}+b_{24})$ and $(-b_{42}+b_{44})$ generally act to decrease the wave height at this location. Therefore, the decrease of K'_R from 1.0 is a little smaller than that calculated by Eq. 129 of the third order theory. The result of numerical calculation for K'_R by the fourth order theory is shown in the lower part of Fig. 9. The comparsion of the lower and upper parts of Fig. 9 indicates the improvement in accuracy is about 0.1 at most in terms of K'_R. The difference of K'_R in Fig. 9 may be taken as a guide to make a better estimate of K_R with Figs. 3 to 8.

3.4 Discussion of the *Subtraction Method*

Murota and Yamada[5] have reported a direct recording of the profile of reflected waves from a sloping board with varying angle in the following way. As shown in Fig. 10, they separated a test channel into two with a partition wall. A model structure for which the reflection coefficient is to be measured is located

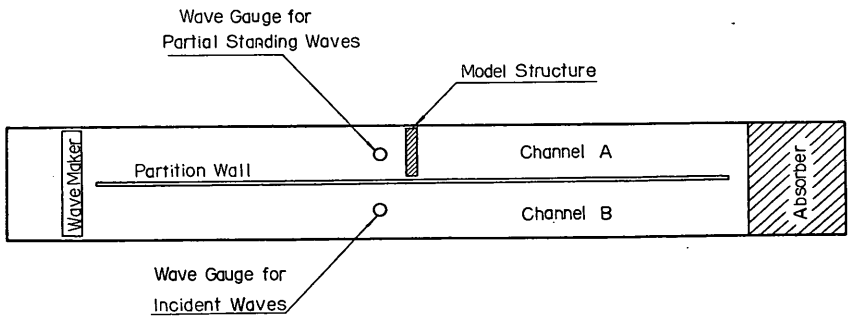

Fig. 10 Channel Arrangement for the *Subtraction Method*

at the center of one channel, A. A parallel-wire resistance type wave gauge is set at an arbitrary distance from the model; the surface displacement of partial standing waves is obtained with this gauge. Another wave gauge is set at the same location of the other channel, B, in order to obtain the surface displacement of incident waves in phase. The output of the gauge B is subtracted in an electric circuit from that of the gauge A so as to yield the surface profile of reflected waves.

This method has two problems to be examined. One problem is the linearity of calibration curves of both the wave gauges and of the subtraction circuit. This is rather of electric performance; hence this will not be discussed in this report though it is important one. The other problem is the applicability of linear operation to partial standing waves. If the partial standing wave system were a simple superposition of incident waves and reflected waves, the subtraction of incident wave profile from partial standing wave profile would yield the profile of reflected waves. As seen in the preceding chapter, however, the incident and reflected waves interfere each other and produce bound waves as well as changes in wavelengths.

If we limit our discussion to the second order approximation or to the case where wave amplitude is not so large, the wavelength of incident and reflected waves is considered unchanged. The difference of surface displacements in the channels A and B is obtained as

$$\eta_{DIF}=\eta_S-\eta_I=a\lambda\varepsilon b_{02}\cos 2k_Ax + \lambda a\{\cos(k_Ax+\sigma t)+\lambda\varepsilon b_{22}\cos 2(k_Ax+\sigma t)\}. \tag{132}$$

The bound waves appear only as the variation of mean water level as indicated by the first term of the above equation. The second term is exactly the expression of reflected waves to the second order approximation; hence the *subtraction method* is justified to this order of approximation.

If the wave amplitude is not so small, the change in wavelength caused by the wave interference effect must be considered in addition to the presence of bound waves. The subtraction of incident waves from the partial standing waves of Eq. 112 yields the following:

$$\eta_{DIF}=\eta_R+\eta_F+\Delta\eta_I, \tag{133}$$

where:

$$\left.\begin{aligned}
\eta_R &= \lambda a\left\{\left(1+\frac{1}{2}\varepsilon^2 b_{11}\right)\cos(k_R x-\sigma t)\right.\\
&\quad \left.+\lambda\varepsilon b_{22}\cos 2(k_R x-\sigma t)+\frac{1}{2}\lambda^2\varepsilon^2 b_{33}\cos 3(k_R x-\sigma t)\right\}\\
\eta_F &= \lambda a b_{02}\cos(k_I-k_R)x+\frac{1}{2}\lambda a\varepsilon^2 b_1\{\lambda\cos(k_I x-\sigma t)+\cos(k_R x-\sigma t)\}\\
&\quad +\frac{1}{2}\lambda a\varepsilon^2 b_{31}\{\cos[(2k_I+k_R)x-3\sigma t]+\lambda\cos[(2k_R+k_I)x-3\sigma t]\}\\
&\quad +\frac{1}{2}\lambda a\varepsilon^2 b_{13}\{\cos[(2k_I-k_R)x-\sigma t]+\lambda\cos[(2k_R-k_I)x-\sigma t]\}\\
\Delta\eta_I &= a\left(1+\frac{1}{2}\varepsilon^2 b_{11}\right)[\cos(k_I x-\sigma t)-\cos(k_I' x-\sigma t)]\\
&\quad +a\varepsilon b_{22}[\cos 2(k_I x-\sigma t)-\cos 2(k_I' x-\sigma t)]\\
&\quad +\frac{1}{2}a\varepsilon^2 b_{33}[\cos 3(k_I x-\sigma t)-\cos 3(k_I' x-\sigma t)],
\end{aligned}\right\} \tag{134}$$

with:

$$\left.\begin{aligned}
k_I' &= k_A\left[1-\frac{1}{2}\varepsilon^2 K_1\right] \quad \text{for incident waves without interference}\\
k_I &= k_A\left[1-\frac{1}{2}\varepsilon^2(K_1-\lambda^2 K_2)\right]\\
&\qquad \text{after interference by reflected waves.}
\end{aligned}\right\} \tag{135}$$

The presence of bound waves η_F increases the height of η_{DIF} by about 15% at most. The magnitude of the effect of bound waves is approximately represented by Eq. 95, which is originally for the increase of standing wave height. The term of $\Delta\eta_I$ represents the effect of wavelength change of incident waves. If the change in wavelength is denoted with Δ_k' or $k_I=k_I'+\Delta_k'$, then $\Delta\eta_I$ is rewritten as

$$\begin{aligned}
\Delta\eta_I &= 2a\left\{\left(1+\frac{1}{2}\varepsilon^2 b_{11}\right)\sin\frac{\Delta_k' x}{2}\cos(k_I x-\sigma t+\theta_1)\right.\\
&\quad +\varepsilon b_{22}\sin\Delta_k' x\cos 2(k_I x-\sigma t+\theta_2)\\
&\quad \left.+\frac{1}{2}\varepsilon^2 b_{33}\sin\frac{3}{2}\Delta_k' x\cos 3(k_I x-\sigma t+\theta_3)\right\}
\end{aligned} \tag{136}$$

where:

$$\left.\begin{aligned}
\Delta_k' &= \frac{1}{2}\lambda^2\varepsilon^2 k_A K_2\\
\theta_n &= \tan^{-1}\left[\frac{\sin n\Delta_k' x}{1-\cos n\Delta_k x}\right]
\end{aligned}\right\} \tag{137}$$

For a small value of x, the following approximation is possible by taking the terms of ε up to the second power

$$\Delta\eta_I \fallingdotseq a\Delta_k' x\cos(k_I x-\sigma t+\theta_1) \tag{138}$$

The above equation shows the increase of the amplituce of $\Delta\eta_I$ with x. This suggests for the *subtraction method* that the wave gauge should be located as near as possible to the source of wave of wave reflection so as to minimize the effect of wavelength change on η_{DIF}. If the deep water waves with $H_I/L_A=0.06$ reflected totally and measured at $x=L$ is considered as an numerical example, the amplitude of $\Delta\eta_I$ is calculated as $0.4a$. The effect of $\Delta\eta_I$ will not be so serious at relatively shallow water as in deep water, because the wavelength change due to wave interference is relatively small at shallow water as expected from Fig. 1. The presence of $\Delta\eta_I$, however, will cause some error in the determination of reflected waves; the value of reflection coefficient greater than 1.0 reported by Murota and Yamada may have been produced by this effect.

4. Experimental Verification of Apparent Reflection Coefficient

4.1 Experimental Apparatus and Test Waves

In order to investigate the validity of the calculation for the apparent coefficient of wave reflection, experiments have been carried out for the reflection coefficient of a vertical wall and energy dissipators of horizontal wire-mesh screens.

A wind-wave channel of 22 m long, 0.6 m wide and 0.8 m deep, glassed in both sides, was used for the test (the wind blower was not used in this test). The channel is equipped with a vertically-oscillating flow type wave generator[15,16] as shown in Fig. 11. The wave paddle is a horizontal plate, which moves up and down in a vertical slot of 40 cm wide. The wave generator has the unique

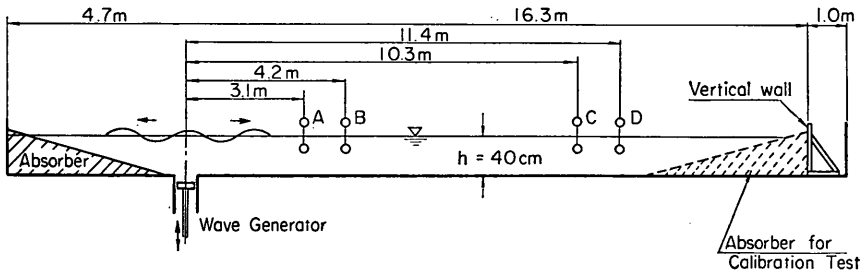

Fig. 11 Sketch of Test Channel

characteristics of non-reflectivity because no vertical member of wave paddle is present. Waves reflected from a model structure placed in the channel pass over the generating area and are dissipated at the wave absorber at the opposite side of the channel. The wave absorber is a mound of milling scraps of stainles steel with a slope of 1 to 10, covered with one layer of crushed stones.

Wave profiles were measured with two wave gauges of capacitance type and recorded on a pen-writing oscillograph. The head of capacitance type gauge is a polyvinyl-formal wire of 25 cm long with the diameter of 0.77 mm; another wire of 30 cm long with the diameter of 0.22 mm was also used for the other wave gauge. The calibration curves of these gauges were linear in the range of ± 10 cm; beyond that a slight non-linearity appeared.

A vertical wall made of painted plywood was set at the distance of 16.3 m

from the center of wave paddle. For the experiment of partial reflection, an energy dissipator composed of horizontal wire mesh screens was placed in front of vertical wall. The screens are made of stainless steel wires of #19 (0.91 mm in diameter) in 5-mesh and stretched to frames of 56 cm × 38 cm, made of 9 mm round bars. With 8 or 15 screens at the average spacing of 5.6 cm or 2.8 cm, the dissipator was 42 cm high, 57 cm wide and 40 cm long. Figure 12 shows the front view of the dissipator.

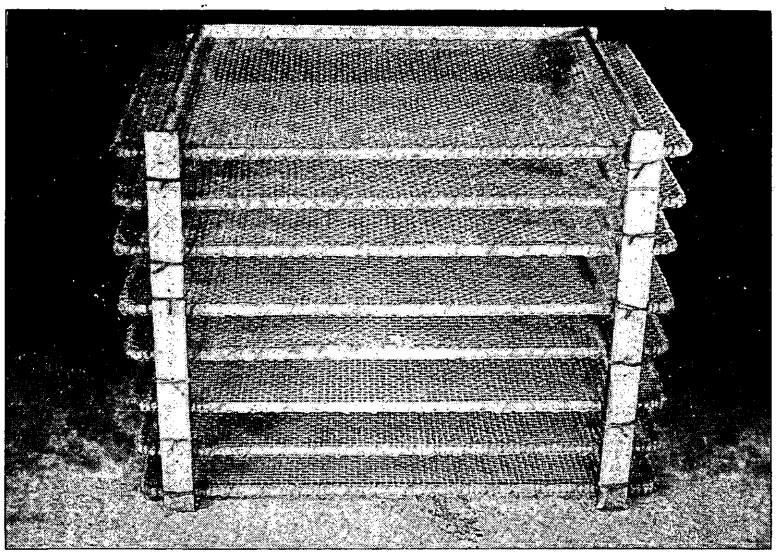

Fig. 12 Front View of Energy Dissipator

The waves employed in the experiments were calibrated before the set-up of the vertical wall. For this measurement, an absorber of milling scraps with the slope of 1 to 10 was placed at the end of channel. Table 1 shows the wave heights measured at the stations of A, B, C and D, shown in Fig. 12 as well as the estimated height of incident wave to the vertical wall. The waves are referred to with the half-stroke of wave paddle e. Each height in Table 1 is the

Table—1 Results of Wave Calibration Test

T (sec)	e (cm)	H (cm) A	B	C	D	H_I (cm)	H_I/L_A
1.25	5.0	4.00	3.55	4.03	3.54	3.67	0.0179
	7.5	5.80	5.45	6.00	5.35	5.48	0.0269
	10.0	7.50	7.75	7.60	7.10	7.26	0.0354
	12.5	9.50	9.25	9.20	9.20	9.04	0.0440
	15.0	11.25	11.35	11.40	11.10	10.90	0.0542
2.15	5.0	2.70	2.50	2.40	2.50	2.43	0.0061
	7.5	4.05	4.10	3.57	4.05	3.79	0.0095
	10.0	5.40	5.15	5.00	4.90	4.91	0.0123
	12.5	6.70	6.45	6.50	6.40	6.26	0.0156
	15.0	8.35	7.90	8.10	8.00	7.77	0.0194

average of 5 runs, each for 10 consecutive waves. Small variations of wave heights at four stations are considered as those inherent in wave tests. Since some decrease of wave height due to frictional damping at side walls and bottom is expected, the incident wave heights were estimated from the distributions of wave heights at A through D with the wave damping being taken into consideration. The period of test waves was set to 1.25 and 2.15 seconds. At the water depth of $h=40$ cm which was kept constant during the experiments, these periods yield the first order wavelengths of $L_A=205$ and 401 cm, or $h/L_A=0.195$ and 0.100.

4.2 Total Wave Reflection from a Vertical Wall

(1) Examination of total reflection by a vertical wall

In the experiment of Greslou and Mahe[8], a vertical wall showed a gradual decrease of reflection coefficient from 1.0 to 0.88 with the increase of deep water wave steepness up to $H_0/L_0=0.05$. Since this is contrary to the concept of total reflection by a vertical wall, the examination of total reflectivity was carried out as the first of the experiments.

The best way to measure the reflection coefficient is to record the reflected waves directly. By making use of non-reflectivity of the wave generator of the channel, we have employed a special method which is described in the following; this will be called the wave tail method in this report. Let us consider the case where we operate the wave generator for a large number of cycle and then switch off. A wave gauge is supposed to be set at A. In the biginning before the wave front is reflected from the vertical wall, there is only the system of incident waves. As the reflected waves come back, the zone of standing waves is extended toward A. Until the arrival of the reflected wave front, the wave record will show a constant wave height, which will be taken as the incident wave height. After the arrival, the wave height changes to that of standing waves, the value of which is dependent upon the phase difference between incident and reflected waves. Since the present wave generator does not reflect the retrogressive waves, the system of standing waves will prevail without change due to re-reflection from the wave paddle. After the generator is switched off, the train of incident waves moves out with the group velocity, leaving the train of reflected waves behind its tail. When the tail of incident wave train arrives at the vertical wall, all the incident waves have been transformed to reflected waves. Hence the wave record at A after the passage of incident wave train can be taken as that of reflected waves.

Since actual wave records show gradual increase of wave heights in the beginning as well as some variations as shown in an example of Fig. 13, the averages of the 3rd to 10th waves for $T=1.25$ seconds and of the 2nd to 5th waves for $T=2.15$ seconds were taken as the incident wave heights. The wave paddle was operated for 50 cycles $T=1.25$ seconds waves and for 30 cycles for $T=2.15$ seconds waves (Fig. 13 is a record of preliminary test for $T=1.25$ seconds waves with 30 cycles operation). At the rear of wave records, the passage of incident waves was clearly recognized by both the change of wave height and the calculation of travel time from the wave generator to the wave gauge. Consecutive records of 10 waves for $T=1.25$ seconds and of 5 waves for $T=2.15$ seconds were utilized to calculate the height of reflected waves. The reflection coefficient was

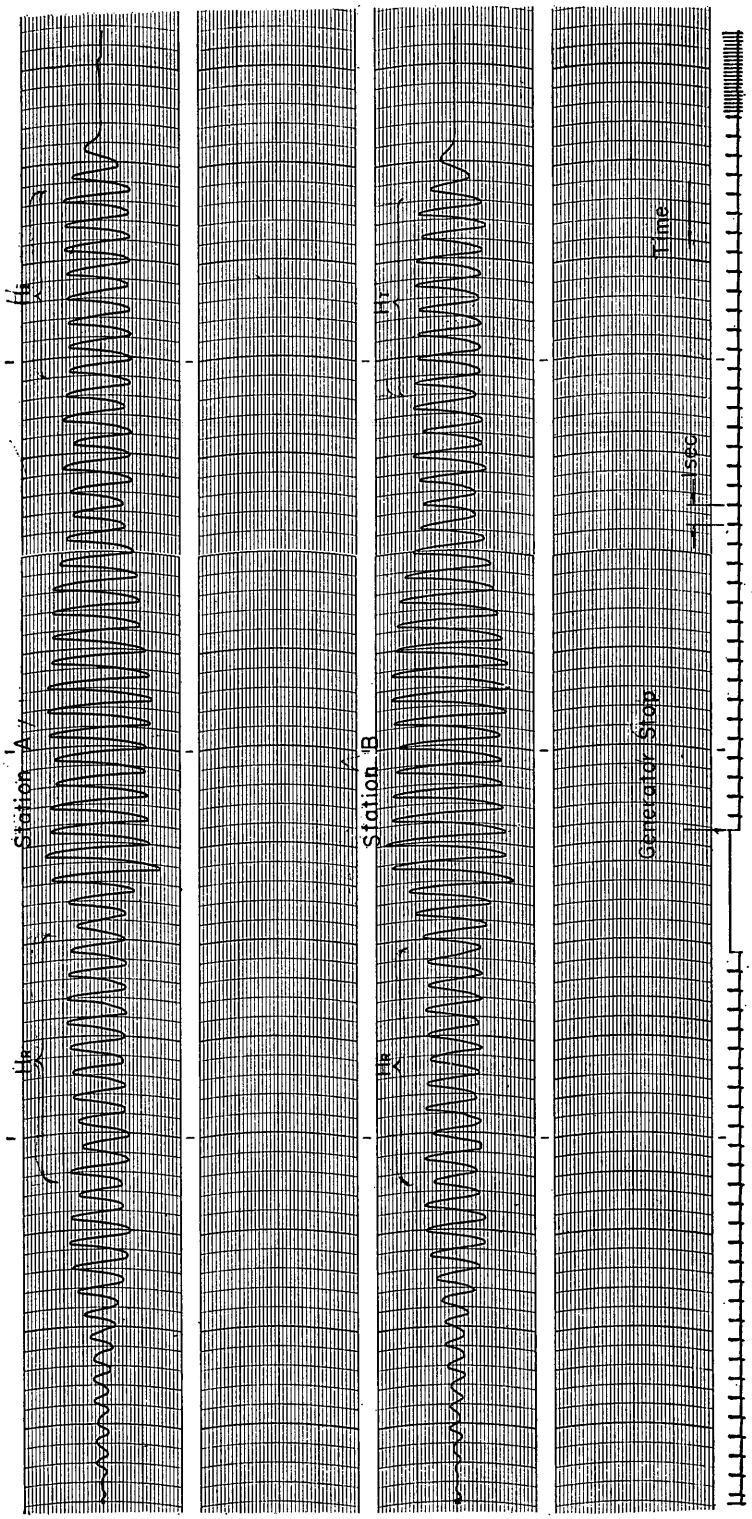

Fig. 13 Example of Oscillograph Record in the Wave Tail Method

then calculated as the ratio of the average height of reflected waves to that of incident waves.

In the present test, wave gauges were set at the stations A and B. The measurement was repeated five times for waves of e=5, 10 and 15 cm with the periods of 1.25 and 2.15 seconds. The average of the reflection coefficient for each wave varied from 0.81 to 0.94 as shown in Table 2. The station B tends to give smaller values than the station A for T=2.15 seconds waves; this seems to have been caused by a small amount of wave reflection from the generating area.

Table—2 Reflection Coefficient of Vertical Wall by Wave Tail Method

T (sec)	e (cm)	$(K_R)_{meas}$ A	$(K_R)_{meas}$ B	H/H_0 A	H/H_0 B	K_R
1.25	5	0.846	0.852	0.910	0.918	0.930
	10	0.856	0.829	0.908	0.916	0.925
	15	0.829	0.941	0.906	0.914	0.973
2.15	5	0.890	0.813	0.943	0.946	0.902
	10	0.849	0.811	0.941	0.945	0.879
	15	0.886	0.825	0.939	0.943	0.908

Note: 1) H/H_0 is for the travel distance of 26.4 m for A and 24.2 m for B.
2) K_R is the average of corrected values at A and B.

The results of Table 2 need to be corrected for the wave height attenuation due to the fricitional damping at the side walls and channel bottom. According to Iwagaki et al[17,18]. The wave height attenuation in a wave channel with the width of B is calculated as

$$H=H_0 \exp(-\epsilon_{b+w}x/L), \tag{139}$$

where:

$$\left.\begin{aligned}
&\epsilon_{b+w}=\frac{4\pi^2}{L}\sqrt{\frac{\nu T}{\pi}}\left(1+\frac{1}{\psi}\right)\Big/(\sinh kh+kh),\\
&\psi\fallingdotseq(kB/\sinh 2kh)\{1-(1.086\,\mathrm{sech}\,kh+0.197)\varepsilon^*\}\\
&\varepsilon^*=(\pi H/L)/\sinh kh\\
&\nu\text{:kinetic viscosity of water.}
\end{aligned}\right\} \tag{140}$$

Since the reflected waves recorded at A and B had traveled twice the distance between the vertical wall and the wave gauges, the attenuation rate of reflected wave height is calculated for the distance of x=26.4 m for A and x=24.2 m for B and is shown in the column of H/H_0 of Table 2. The effect of wave amplitude represented with the term of ε^* is shown to be very small in the present test. The measured values of reflection coefficient are then divided with the attenuation rate of H/H_0 so as to yield the actual reflection coefficient of the vertical wall, which is listed as K_R in Table 2. By this procedure, the reflection coefficient was estimated as K_R=0.90 for T=2.15 second waves and K_R=0.94 for

T=1.25 seconds waves regardless of the wave amplitude. These values of reflection coefficient smaller than 1.0 seems to have appeared by the insufficient correction for wave attenuation. The actual wave attenuation in a wave channel is reported to be larger than the calculated value of Eq. 139 by the amount of 20 to 30% in the average in terms of ϵ_{b+w}[17,18]; some data show the value of more than twice the calculated one. The distribution of incident wave heights listed in Table 1 suggests the stronger attenuation for T=2.15 seconds waves than for T=1.25 seconds waves, even though the calculation by Eq. 139 predicts the opposite. The irregularity of side walls at the junctions between the glasses and supporting frames is also considered to have caused additional damping. Therefore, the vertical wall tested can be regarded to have the reflection coefficient very near to 1.0.

(2) Apparent reflection coefficient of a vertical wall

The reflection coefficient of the vertical wall was also measured with the conventional method of Healy's one. A wave gauge was fixed at the distance of 1 cm from the wall for the measurement of H_{max} and another gauge was set around the first nodal point of a quater wavelength from the wall for the measurement of H_{min}. The latter gauge wave moved every 1 cm in the range of $\pm$3 cm from the quater-wavelength point. The wave height at each location was calculated from the record as the average of consecutive 10 waves, and the minimum value of average wave height among the measured heights around the nodal point was taken as H_{min}. The wave height in front of the wall was taken as H_{max}. The apparent heights of incident and reflected waves were then calculated by Eq. 101 and the apparent reflection coefficient by Eq. 102. The results are listed in Table 3.

Table—3 Apparent Reflection Coefficient of Vertical Wall by Healy's Method

e (cm)	T=1.25 sec			T=2.15 sec		
	H_{max} (cm)	H_{min} (cm)	K'_R	H_{max} (cm)	H_{min} (cm)	K'_R
5.0	6.90	0.68	0.821	4.70	0.51	0.804
7.5	11.20	0.75	0.874	7.00	0.93	0.765
10.0	14.65	1.55	0.809	9.55	1.50	0.729
12.5	17.65	2.31	0.769	12.70	2.27	0.697
15.0	23.46	2.75	0.790	14.85	2.75	0.688

It is seen in Table 3 that the apparent reflection coefficient decreases as the wave amplitude increases; the decrease is greater for T=2.15 seconds than for T=1.25 seconds. This tendency is well predicted with the present theory as shown in Fig. 14, where the data of K'_R are compared with the calculated values for the case of total reflection (In the range of wave steepness tested, the third and fourth order theories give almost the same value of K'_R). The increase of apparent incident wave height also agrees with the theory as shown in Fig. 15, although the data show some scatter owning to the difficulty to estimate the height of incident wave accurately. The increase of standing wave height pre-

dicted by Eq. 95 could not be recognized clearly, possibly because of the small amount of increase for the range of experimental condition.

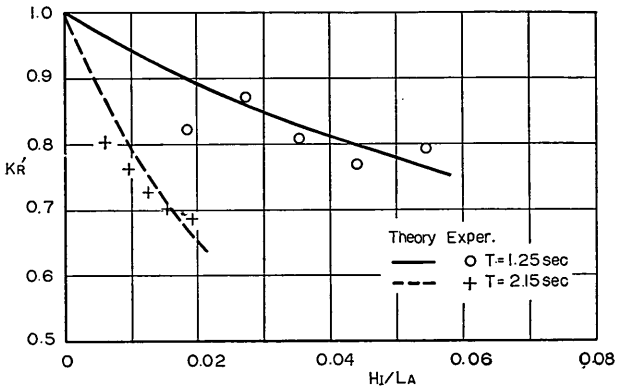

Fig. 14 Apparent Reflection Coefficient of a Vertical Wall: Theory and Experiment

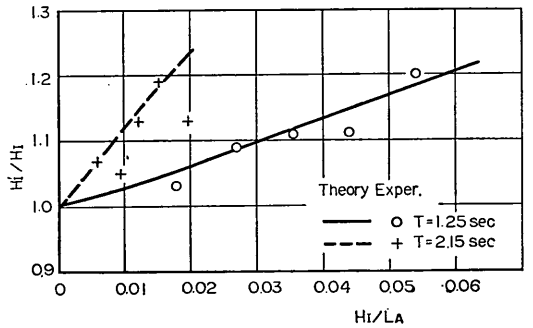

Fig. 15 Increase of Apparent Incident Wave Height

Another verification of the theory is exhibited in Fig. 16, where the wave records at different locations are compared. As the wave gauge is moved from the front of the wall (x=1 cm) toward the nodal point, the second harmonic oscillation becomes visible. The records at x=50 cm for T=1.25 seconds and at x=100 cm for T=2.15 seconds have been transformed into twice frequency oscillations. Figure 17 shows the variation of wave height with respect to the distance from the wall for the waves shown in Fig. 16. The solid lines represent the theoretical envelopes for the incident wave heights listed in Table 1. The wave envelopes by the small amplitude wave theory are shown with dash-dot lines. For the case shown in this figure, the difference between the finite and small amplitude theories is small except for the neightbourhood of the nodal point. The experimental data, however show better agreement with the finite amplitude theory than with the small amplitude theory.

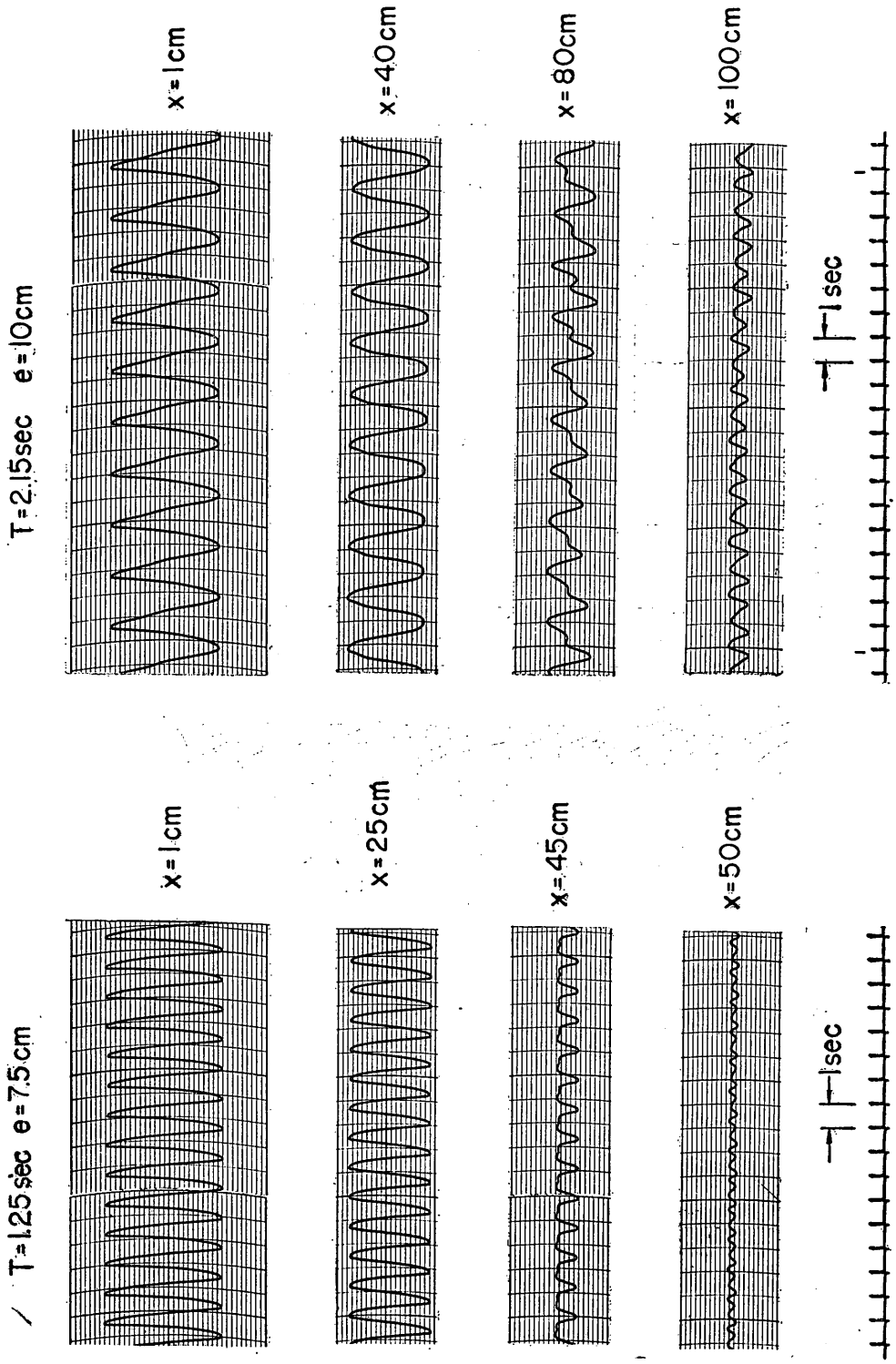

Fig. 16 Wave Profiles at Various Locations in front of a Vertical Wall

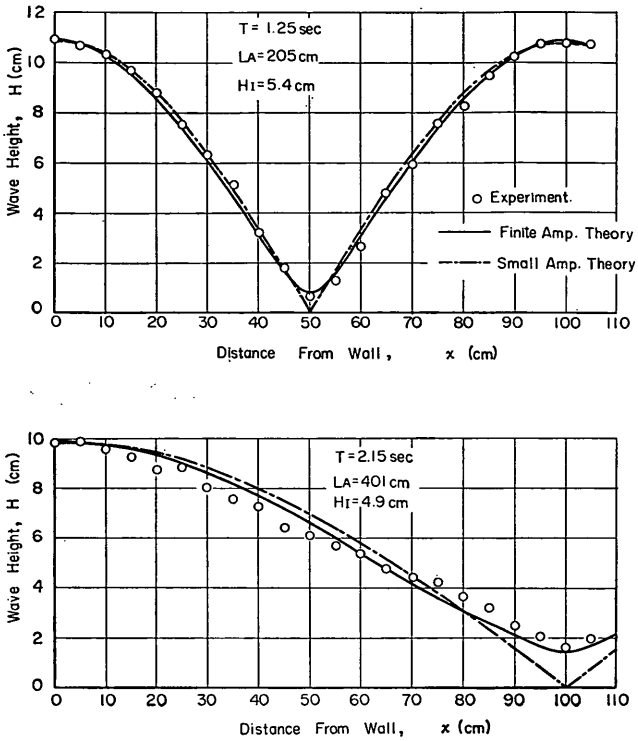

Fig. 17 Variation of Wave Height in front of a Vertical Wall

4.3 Partial Wave Reflection from Energy Dissipator

Tests were also made for the case of partial wave reflection from the energy dissipator described in Section 4.1. Wave of T=1.25 and 2.15 seconds for e=5, 10, 15 cm were employed in the test.

First the wave tail method was applied in order to investigate the actual value of reflection coefficient of the energy dissipator. Two wave gauges were

Table—4 Reflection Coefficient of Wave Dissipator by Wave Tail Method

T (sec)	e (cm)	With 8 screens			With 15 screens		
		A	B	K_R	A	B	K_R
1.25	5	0.681	0.670	0.740	0.562	0.553	0.610
	10	0.539	0.523	0.658	0.471	0.484	0.524
	15	0.504	0.543	0.576	0.361	0.419	0.428
2.15	5	0.919	0.822	0.922	0.880	0.746	0.861
	10	0.877	0.726	0.849	0.768	0.752	0.806
	15	0.811	0.731	0.818	0.751	0.703	0.772

Note: 1) Colums of A and B list the measured values of K_R at the stations A and B.
2) K_R is the average of corrected values at A and B.

set at the stations A and B, and the wave records were analysed in the same way as described before. The results are shown in Table 4. As for the case of total reflection, the reflection coefficient listed in Table 4 has been corrected for the wave attenuation with the ratio of H/H_0 listed in Table 2 and averaged for the stations A and B. Although the attenuation rate of Table 2 is considered to be smaller than the actual value, the absence of positive data for the appropriate correction supported the adoption of the above value. Different from the case of vertical wall, the reflection coefficient of the energy dissipator employed decreases as the wave amplitude increases. Such a tendency is considered as characteristic to the energy dissipator of screen types, since a similar tendency has been reported for the dissipator composed of vertical screens with theoretical analysis[19].

The reflection coefficient of the energy dissipator was then measured by means of Healy's method. The measurement was carried out in the same way as described in the previous section; this time, the wave gauge for H_{max} was stationed at the second anti-node of a half wavelength away from the vertical wall. Table 5 lists the result of measurement. It is seen from the comparison of Tables 4

Table—5 Reflection Coefficient of Wave Dissipator by Healy's Method

T (sec)	e (cm)	With 8 screens				With 15 screens			
		H_{max} (cm)	H_{min} (cm)	K'_R	$(K_R)_{est.}$	H_{max} (cm)	H_{min} (cm)	K'_R	$(K_R)_{est.}$
1.25	5	6.81	0.87	0.773	0.78	5.88	1.46	0.602	0.60
	10	12.48	2.08	0.716	0.75	11.34	3.47	0.531	0.52
	15	18.18	4.99	0.570	0.56	15.99	6.06	0.449	0.42
2.15	5	4.44	0.52	0.790	0.84	4.20	0.63	0.739	0.77
	10	9.13	1.57	0.706	0.86	9.08	1.69	0.686	0.80
	15	13.57	2.99	0.639	0.87	12.24	3.18	0.588	0.75

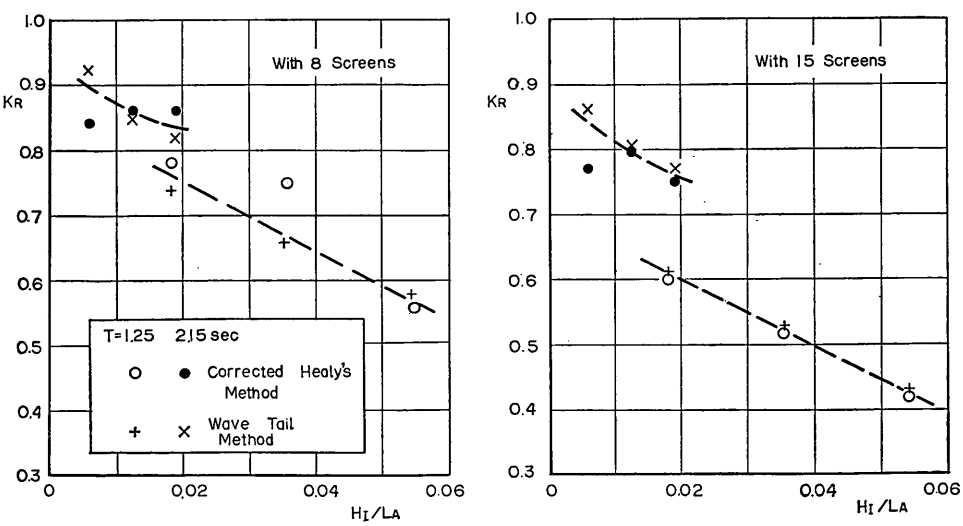

Fig. 18 Reflection Coefficient of Screen Type Energy Dissipator

and 5 that the apparent reflection coefficient for the waves of T=1.25 seconds is almost the same with the actual reflection coefficient estimated by the wave tail method, while the apparent coefficient for the waves of T=2.15 seconds is much smaller than that by the wave tail method. Referring to Fig. 2, this is explained as such that the reflection coefficient of T=1.25 seconds belongs to the region of $K_R' \fallingdotseq K_R$, while the data of T=2.15 seconds waves belongs to the region of $K_R' < K_R$. The apparent reflection coefficients of Table 5 were then plotted in figures similar to Figs. 4 and 7 in order to estimate the true values of reflection coefficient by interpolation. The reflection coefficients of the energy dissipator thus estimated are listed in Table 5 as $(K_R)_{est}$ and shown in Fig. 18 against the wave steepness. The reflection coefficient by the wave tail method and that by the corrected Healy's method for finite amplitude effect are seen to agree each other in Fig. 18; the difference is less than 0.09 in terms of K_R. The agreement is a good indication of the validity of the present theory.

Another test of the present theory has been made for the estimation of incident wave height. Since the apparent incident wave heights are calculated by Eq. 101 in Healy's method, they are listed as H_I' in Table 6 for all the experimental data. The estimation of incident wave height is also possible with the aid of Figs. 3 to 8 from the data of K_R' and H_I' without any knowledge on K_R and H_I. The estimation has been made for the same data and the results are listed in Table 6 as $(H_I)_{est}$. Another estimation on the basis of standing wave height with the aid of Eq. 95 has been made, too, as shown in the last column of Table 6. It is clear in Table 6 that the estimated heights of incident waves $(H_I)_{est}$ are almost the same with those by wave calibration test, whereas the values of H_I' themselves deviate from H_I with the increase of the reflection coefficient or with the increase of wave steepness. The result of Table 6 shows that the incident wave height if calculated by Healy's method should be corrected

Table—6 Apparent and Estimated Heights of Incident Waves

T (sec)	e (cm)	H_I[1] (cm)	H_I' (cm)			$(H_I)_{est.}$ (cm)			
			(1)	(2)	(3)	(1)	(2)	(3)	(4)
1.25	5.0	3.67	3.79	3.84	3.67	3.71	3.80	3.67	3.43
	7.5	5.48	5.97	—	—	5.55	—	—	5.53
	10.0	7.26	8.10	7.26	7.40	7.29	6.98	7.38	7.18
	12.5	9.04	9.98	—	—	8.79	—	—	8.56
	15.0	10.90	13.05	11.04	11.02	11.05	10.72	10.98	11.19
2.15	5.0	2.43	2.60	2.48	2.42	2.50	2.41	2.39	2.35
	7.5	3.79	3.97	—	—	3.67	—	—	3.48
	10.0	4.91	5.53	5.35	5.38	4.93	4.86	4.98	4.74
	12.5	6.26	7.49	—	—	6.29	—	—	6.25
	15.0	7.77	8.80	8.28	7.71	7.30	7.14	7.08	7.27

Note: 1) Incident wave height estimated in wave calibration test and listed in Table 1.
2) (1), (2) and (3) represent the cases of no dissipator, dissipator with 8 screens, and that with 15 screens, respectively.
3) (4) represents $(H_I)_{est.}$ from the data of standing wave heights.

for the finite amplitude effect with the aid of Figs. 3 to 8 or by numerical calculation. A simple use of Eq. 101 for incident wave height will result in an overestimation of considerable magnitude if the reflection coefficient of a test structure belongs to the region of $K_R' < K_R$ shown in Fig. 2.

5. Conclusions

From the theoretical analysis and experimental investigation described herein, the following conclusions can be made:

1) The interaction of progressive and retrogressive waves of finite amplitudes causes the shortening of wavelengths and increase of wave heights for both waves. The standing wave height is therefore a little larger than twice the incident wave height.

2) The nodal point of standing waves has the oscillation of twice frequency, chiefly owning to the second harmonic component of incident waves of finite amplitude.

3) The presence of the higher harmonics in incident waves and the formation of bound waves by the wave interaction nulify the validity of Healy's method for the measurement of reflection coefficient for a structure of high reflectivity.

4) The resolution of incident and reflected waves from a partial standing wave system by means of Healy's method should be done with due correction for the finite amplitude effect; Figs. 3 to 8 will fascillitate the procedure of correction.

Acknowledgements

The authors wish to express their thanks to Dr. Tokuichi Hamada for his critical review of the manuscript. The experimental phase of the study was undertaken by Yoshiyuki Abe with the assistance of Mr. Toshio Fukumori, and the theoretical work as well as the preparation of the report was done by Yoshimi Goda. The numerical computation has been carried out with the aid of a digital computer TOSBAC 3400 at the Computation Center of the Institute.

References

1) IPPEN, A. T. (ed.): "*Estuary and Coastline Hydrodynamics*," McGraw-Hill, Inc., New York, 1966, pp. 384-395.

2) HEALY, J. J.: "Wave Damping Effect of Beaches," *Proc. Minnesota International Hydraulics Convention*, 1953, pp. 213-220.

3) GRESLOU, L. and MAHE, Y.: "Étude du Coefficient de Réflexion d'une Houle sur un Obstacle Constitute par an Plan Incline," *Proc. Fifth Conf. on Coastal Eng.*, Grenoble, 1954, pp. 68-83.

4) GODA, Y. and KAKIZAKI, S.: "Study on Finite Amplitude Standing Waves and Their Pressures upon a Vertical Wall (*in Japanese*)," *Report of Port and Harbour Research Institute*, Vol. 5, No. 10, 1966, p. 16.

5) MUROTA, A. and YAMADA, T.: "A Fundamental Study on Wave Reflection (*in Japanese*)," *Proc. 13th Conf. on Coastal Eng. in Japan*, 1966, pp. 9-14.

6) JAMES, W.: "Resolution of Partial Clapotis," *Detailed Summaries of Tenth Conf. on Coastal Eng.*, Tokyo, Ex-2.
7) SKJELBREIA, L and HENDRICKSON, J.: "Fifth Order Gravity Wave Theory," *Proc. Seventh Conf. on Coastal Eng.*, Hague, 1960, pp. 184-196.
8) CHAPPELEAR, J. H.: "Direct Numerical Calculation of Wave Properties," *J. Geophys. Res.*, Vol. 66, No. 2, 1961, pp. 501-508.
9) DEAN, R. G.: "Stream Function Wave Theory; Validity and Application," *Santa Barbara Coastal Eng. Conf.*, 1965, pp. 269-299.
10) TADJBAKSH, I. and KELLER, J. B.: "Standing Surface Waves of Finite Amplitude," *J. Fluid Mech.*, 8, 1960, pp. 442-451.
11) HAMADA, T.: "The Secondary Interactions of Surface Waves," *Report of Port and Harbour Research Institute*, No. 10, 1965, 28pp.
12) LONGUET-HIGGINS, M. S. and PHILLIPS, O. M.: "Phase Velocity Effects in Tertiary Wave Interaction," *J. Fluid Mech.*, **12**, 1962, pp. 333-336.
13) FULTZ, D.: "An Experimental Note on Finite Amplitudes Standing Gravity Waves," *J. Fluid Mech.*, **13**, 1962, pp. 193-212.
14) GODA, Y.: "The Fourth Order Approximation to the Pressure of Standing Waves," *Coastal Engineering in Japan, JSCE*, Vol. 10, 1967, pp. 1-11.
15) GODA, Y. and KIKUYA, T.: "The Generation of Water Waves with a Vertically Oscillating Flow at a Channel Bottom," *Report of Port and Harbour Research Institute*, No. 9, 1964, 24pp.
16) HIROMOTO, F., ABE, Y. and SUDO, S.: "On the Design of Vertically Oscillating Flow Type Wave Generator (*in Japanese*)," *Tech. Note of Port and Harbour Research Institute*, No. 32, 1967, pp. 81-97.
17) IWAGAKI, Y., TSUCHIYA, Y. and CHIN, H.: "Basic Studies on the Wave Damping Due to Bottom Friction (3)—Effect of non-linear terms in the equations of laminar boundary layer—(*in Japanese*)," *Proc. 12th Conf. on Coastal Eng. in Japan*, 1965, pp. 41-49.
18) IWAGAKI, Y. and TSUCHIYA, Y.: "Laminar Damping of Oscillatory Waves due to Bottom Friction," *Proc. Tenth Conf. on Coastal Eng.*, Tokyo, 1966, pp. 149-174.
19) GODA, Y. and IPPEN A. T.: "Theoretical and Experimental Investigation of Wave Energy Dissipators Composed of Wire Mesh Screens," *Report of Hydrodynamics Laboratory, Massachusetts Inst. of Technology*, No. 60, 1963, 66pp.

List of Symbols

a : first order amplitude of surface elevation
$A_n^{(r)}$: time function for the $(r+1)$th order perturbation of velocity potential
b_{mn} : coefficient of elevation
B : width of channel
$B_n^{(r)}$: time function for the $(r+1)$th order perturbation of velocity potential
c : abbreviation for $\coth kh$ (Eq. 42 or 75)
C_1 : correction factor to wave frequency due to finite amplitude effect of progressive waves (Eq. 52)
C_2 : correction factor to wave frequency due to third order interaction between progressive and retrogressive waves (Eq. 85)
e : half-stroke of wave paddle
g : acceleration of gravity ($=980\,\mathrm{cm/sec^2}$)
h : water depth
H : wave height in general
H_I : incident wave height
H_I' : apparent incident wave height calculated by Healy's method (Eq. 101)
H_0 : deep water wave height or initial wave height
H_R : reflected wave height
H_R' : apparent reflected wave height calculated by Healy's method (Eq. 101)
k : wavh number in general ($=2\pi/L$)
$\bar{k}$: average of incident and reflected wave numbers (Eq. 113)
K_1 : correction factor to wave number corresponding to C_1 (Eq. 60)
K_2 : correction factor to wave number corresponding to C_2 (Eq. 91)
K_R : reflection coefficient ($=H_R/H_I$)
K_R' : apparent reflection coefficient calculated by Healy's method (Eq. 102)
L : wavelength in general
n : integer (0, 1, 2, $\cdots$)
r : integer (0, 1 or 2)
t : time
T : wave period
x : horizontal coordinate
y : vertical coordinate measured upward from the still water level
$-^{(r)}$: superscript referring to the $(r+1)$th order perturbation
$-_A$: subscript referring to the value of small amplitude wave
$-_F$: subscript referring to bound waves
$-_I$: subscript referring to incident waves
$-_R$: subscript referring to reflected waves
$-_S$: subscript referring to standing waves
α : coefficient of non-periodic term of velocity potential
β_{mn} : coefficient of velocity potential
Δ_k : difference in wave number (Eq. 115)
ε : parameter related to wave amplitude ($=ka$)
ε^* : parameter related to amplitude effect in frictional damping (Eq. 140)
ϵ_{b+w} : wave height attenuation factor (Eq. 140)
η : vertial displacement of the water surface measured from $y=0$
θ : phase angle

λ : ratio of retrogressive to progressive wave amplitudes in the first order approximation
ν : kinetic viscosity of water
π : constant (3.14159···)
σ : angular wave frequency ($2\pi/T$)
$\sigma_0, \sigma_1, \sigma_2$: first, second, and third order perturbation to angular wave frequency
τ : non-dimensional time (Eq. 10)
Φ : velocity potential
ϕ : channel width factor in frictional damping (Eq. 140)

Appendix: FORTRAN PROGRAM for the Calculation of Pratial Standing Waves

```
 FORTRAN  LIST  66/12

 1    10000   C  SURFACE PROFILE OF PARTIAL STANDING WAVES
 2    10000   C                                                  APRIL  1968, Y.GODA
              C  PROGRAM UNITS(3),  MAIN, EPSLON AND HEIGHT
 3    10000   C
 4    10000        DIMENSION REF(10),X(12),DX(12),T(38),COS2D(12),SIN2D(12)
                1    COS1T(37),COS2T(37),COS3T(37),SIN1T(37),SIN2T(37),SIN3T(37),
                2    COS1X(12),COS2X(12),COS3X(12),SIN1X(12),SIN2X(12),SIN3X(12),
                3    SURFEL(37,12),HT(12),AKX(12)
 5    10000        DIMENSION H(21)
 6    10000   C
 7    10000        READ 1000,(X(M),M=1,12)
 8    10025   1000 FORMAT(12F5.2)
 9    10025    100 DO 101 M=1,12
10    10027        AKX(M)=3.14159265*X(M)/180.
11    10045        COS1X(M)=COSF(AKX(M))
12    10062        COS2X(M)=2.*COS1X(M)**2-1.
13    10102        COS3X(M)=4.*COS1X(M)**3-3.*COS1X(M)
14    10132        SIN1X(M)=SINF(AKX(M))
15    10147        SIN2X(M)=2.*COS1X(M)*SIN1X(M)
16    10172        SIN3X(M)=-4.*SIN1X(M)**3+3.*SIN1X(M)
17    10223    101 CONTINUE
18    10233        T(1)=0.0
19    10240    102 DO 103 L=1,37
20    10242        COS1T(L)=COSF(T(L))
21    10257        COS2T(L)=2.*COS1T(L)**2-1.
22    10277        COS3T(L)=4.*COS1T(L)**3-3.*COS1T(L)
23    10327        SIN1T(L)=SINF(T(L))
24    10344        SIN2T(L)=2.*SIN1T(L)*COS1T(L)
25    10367        SIN3T(L)=-4.*SIN1T(L)**3+3.*SIN1T(L)
26    10420        T(L+1)=T(L)+6.2831853/36.
27    10436    103 CONTINUE
28    10446   C
29    10446        READ 1001, KREF
30    10454   1001 FORMAT(I2)
31    10454        READ 1002,(REF(I),I=1,KREF)
32    10501      1 READ 1003, DLA,HLA,DELHLA,KHLA
33    10515        IF(DLA) 99,99,2
34    10521   1002 FORMAT(10F5.2)
35    10521   1003 FORMAT(3F10.5,I10)
36    10521   2000 FORMAT(1H1,91HSURFACE PROFILE OF PARTIAL STANDING WAVES ///)
37    10521   C
38    10521      2 TANH1=TANHF(6.2832*DLA)
39    10525        PRINT 1000,(X(M),M=1,12)
40    10552        PRINT 1001,KREF
41    10560        PRINT 1002,(REF(I),I=1,KREF)
42    10605        PRINT 1003,DLA,HLA,DELHLA,KHLA
43    10621        TANH2=TANH1**2
44    10625        COTH1=1./TANH1
45    10630        COTH2=COTH1**2
46    10634        COTH4=COTH2**2
47    10640        B02=(TANH1+COTH1)*0.5
48    10644        B11=(3.*COTH4+8.*COTH2-9.)/8.
49    10655        B22=COTH1*(3.*COTH2-1.)/4.
50    10663        B33=(9.*COTH2*COTH4-3.*COTH4+3.*COTH2-1.)*3./32.
51    10702        B1=(-COTH2+2.+TANH2)/4.
52    10710        B31=(-3.*COTH4-18.*COTH2+5.)/32.
```

```
53    10722        B13=(9.*COTH4+27.*COTH2-15.+TANH2+2.*TANH2**2)*3./32.
54    10743        AK1=(9.*COTH4-10.*COTH2+9.)/4./(1.+6.2832*DLA*(COTH1-TANH1))
55    10763        AK12=(9.*COTH4-8.*COTH2+21.+2.*TANH2)/(1.+6.2832*DLA*(COTH1-TANH1)
                  1      )/32.
56    11007        H(1)=HLA
57    11014  C
58    11014    200 DO 201 J=1,KHLA
59    11016        HLA=H(J)
60    11025        E=EPSLON(3.14159*HLA,(B11+B33+AK1)*0.5)
61    11041        EE=E*E
62    11044    300 DO 301 I=1,KREF
63    11046        EL=EPSLON(3.14159*HLA*REF(I),(B11+B33+AK1)*0.5)
64    11070        ALAM=EL/E
65    11073        AK3=AK12*EE*(1.-ALAM**2)
66    11103     20 DO 21 M=1,12
67    11105        DX(M)=-2.*AK3*AKX(M)
68    11124        COS2D(M)=COSF(DX(M))
69    11141        SIN2D(M)=SINF(DX(M))
70    11156     21 CONTINUE
71    11166  C
72    11166        PRINT 2000
73    11172        PRINT 2001,DLA,HLA,REF(I),E,ALAM,AK3
74    11217        PRINT 2002,(X(M),M=1,12)
75    11244  2001 FORMAT( 5X,6HD/LA = F7.4,5X,6HH/LA = F7.4,5X,6HREFK = F7.4, 8X,
                  1            3HE = F7.4,5X,6HALAM = F7.4,5X,6H AK3 = F8.5 ///)
76    11244  2002 FORMAT( 5X,7HT(DEG) , 12(4H  X=F5.1) //)
77    11244  2003 FORMAT( 5X,F5.1,2X,12F9.4)
78    11244  8000 FORMAT(1H )
79    11244  C
80    11244        AP1=1.+ALAM
81    11247        AP2=1.+ALAM**2
82    11254        AP3=1.+ALAM**3
83    11261        AN1=1.-ALAM
84    11264        AN2=1.-ALAM**2
85    11272        AN3=1.-ALAM**3
86    11300  C
87    11300        DEG=0.0
88    11302        DELDEG=10.
89    11304     30 DO 31 L=1,37
90    11306        IF(L-7) 40,6,7
91    11313      7 IF(XMODF(L-1,6)) 40,6,40
92    11322      6 PRINT 8000
93    11326     40 DO 41 M=1,12
94    11330        SURFEL(L,M)=AP1*COS1X(M)*COS1T(L)+AN1*SIN1X(M)*SIN1T(L)
                  1             +E*B22*(AP2*COS2X(M)*COS2T(L)+AN2*SIN2X(M)*SIN2T(L))
                  2             +E*B02*COS2X(M)
95    11446        SURFEL(L,M)=SURFEL(L,M)+0.5*EE
                  2           *(B11*(AP3*COS1X(M)*COS1T(L)+AN3*SIN1X(M)*SIN1T(L))
                  3            +B33*(AP3*COS3X(M)*COS3T(L)+AN3*SIN3X(M)*SIN3T(L)))
96    11564        SURFEL(L,M)=SURFEL(L,M)+0.5*EE*B31*ALAM
                  4            *(AP1*COS1X(M)*(COS3T(L)*COS2D(M)-SIN3T(L)*SIN2D(M))
                  5             +AN1*SIN1X(M)*(SIN3T(L)*COS2D(M)+COS3T(L)*SIN2D(M)))
97    11714        SURFEL(L,M)=SURFEL(L,M)+0.5*EE*B13*ALAM
                  6            *(AP1*COS3X(M)*(COS1T(L)*COS2D(M)+SIN1T(L)*SIN2D(M))
                  7             +AN1*SIN3X(M)*(SIN1T(L)*COS2D(M)-COS1T(L)*SIN2D(M)))
98    12044        SURFEL(L,M)=SURFEL(L,M)+0.5*EE*B1*ALAM
                  8           *(AP1*COS1X(M)*COS1T(L)-AN1*SIN1X(M)*SIN1T(L))
99    12124        SURFEL(L,M)=SURFEL(L,M)/(1.+0.5*EE*(B11+B33))
100   12153     41 CONTINUE

101   12163        PRINT 2003,DEG,(SURFEL(L,M),M=1,12)
102   12214        DEG=DEG+DELDEG
103   12217     31 CONTINUE
104   12227  C
105   12227     50 DO 51 M=1,12
106   12231        HT(M)=HEIGHT(37,M,SURFEL)
107   12243     51 CONTINUE
108   12253        PRINT 2004,(HT(M),M=1,12)
109   12300        REFK1=(HT(1)-HT(2))/(HT(1)+HT(2))
110   12323        REFK2=(HT(11)-HT(2))/(HT(11)+HT(2))
111   12346        REFK3=(HT(11)-HT(12))/(HT(11)+HT(12))
112   12371        PRINT 2005,REFK1,REFK2,REFK3
113   12403  2004 FORMAT(1H0,3X,8HHEIGHT =,12F9.4)
114   12403  2005 FORMAT(1H0,10X,7HREFK1 =,F7.4,32X,7HREFK2 =,F7.4,32X,7HREFK3 =,
                  1                                                      F7.4)
115   12403    301 CONTINUE
116   12413        H(J+1)=H(J)+DELHLA
117   12430    201 CONTINUE
118   12440        GO TO 1
119   12441     99 CALL EXIT
120   12442        END(0,1,0,0,0)
```

```
      141    12442          FUNCTION EPSLON(A,B)
      142    12450          X1=A
      143    12452        1 X2=X1-(B*X1**3+X1-A)/(3.*B*X1**2+1.)
      144    12473          IF(X2-0.9999*X1) 2,3,3
      145    12502        2 X1=X2
      146    12504          GO TO 1
      147    12505        3 EPSLON =X2
      148    12507          RETURN
      149    12511          END(0,1,0,0,0)
      150    12520          FUNCTION HEIGHT(N,M,S)
      151    12526    C
      152    12526          DIMENSION S(37,12)
      153    12526    C
      154    12526          SMAX=-1.0E+100
      155    12531          SMIN=+1.0E+100
      156    12533       10 DO 11 I=1,N
      157    12535          IF(S(I,M)-SMAX) 3,3,2
      158    12551        2 SMAX=S(I,M)
      159    12562        3 IF(S(I,M)-SMIN) 4,4,11
      160    12576        4 SMIN=S(I,M)
      161    12607       11 CONTINUE
      162    12617          HEIGHT=SMAX-SMIN
      163    12622          RETURN
      164    12624          END(1,0,0,0,0)
PROCESSING COMPLETE     OBJECT PROGRAM  02641
```

SURFACE PROFILE OF PARTIAL STANDING WAVES

D/LA = 0.1000 H/LA = 0.0123 REFK = 0.6000 E = 0.0375 ALAM = 0.6110 AK3 = 0.00139

T(DEG)	X= 0.	X= 90.0	X=100.0	X=110.0	X=120.0	X=130.0	X=140.0	X=150.0	X=160.0	X=170.0	X=180.0	X=270.0
0.	1.8506	-0.2394	-0.4827	-0.6949	-0.8762	-1.0279	-1.1512	-1.2473	-1.3162	-1.3578	-1.3717	-0.2394
10.0	1.8118	-0.1686	-0.4205	-0.6415	-0.8306	-0.9888	-1.1177	-1.2185	-1.2919	-1.3380	-1.3567	-0.2865
20.0	1.6985	-0.0756	-0.3311	-0.5582	-0.7543	-0.9194	-1.0541	-1.1600	-1.2378	-1.2883	-1.3115	-0.3114
30.0	1.5190	0.0349	-0.2171	-0.4460	-0.6472	-0.8185	-0.9595	-1.0708	-1.1535	-1.2085	-1.2363	-0.3174
40.0	1.2857	0.1553	-0.0840	-0.3083	-0.5105	-0.6861	-0.8328	-0.9501	-1.0383	-1.0984	-1.1311	-0.3097
50.0	1.0140	0.2756	0.0599	-0.1509	-0.3477	-0.5237	-0.6746	-0.7971	-0.8913	-0.9572	-0.9957	-0.2938
60.0	0.7201	0.3849	0.2044	0.0178	-0.1649	-0.3649	-0.4856	-0.6121	-0.7121	-0.7846	-0.8299	-0.2750
70.0	0.4193	0.4724	0.3382	0.1874	0.0295	-0.1260	-0.2704	-0.3971	-0.5012	-0.5803	-0.6335	-0.2581
80.0	0.1248	0.5289	0.4504	0.3464	0.2246	0.0942	-0.0354	-0.1560	-0.2609	-0.3454	-0.4072	-0.2464
90.0	-0.1531	0.5485	0.5318	0.4838	0.4090	0.3150	0.2104	0.1041	0.0043	-0.0828	-0.1560	-0.2426
100.0	-0.4073	0.5289	0.5762	0.5901	0.5714	0.5245	0.4559	0.3738	0.2867	0.2018	0.1249	-0.2465
110.0	-0.6336	0.4724	0.5814	0.6591	0.7026	0.7111	0.6889	0.6414	0.5759	0.4997	0.4194	-0.2581
120.0	-0.8300	0.3850	0.5493	0.6884	0.7951	0.8651	0.8976	0.8938	0.8590	0.7990	0.7202	-0.2751
130.0	-0.9958	0.2756	0.4859	0.6798	0.8471	0.9792	1.0706	1.1176	1.1216	1.0853	1.0141	-0.2938
140.0	-1.1312	0.1553	0.4000	0.6389	0.8596	1.0201	1.1998	1.3009	1.3488	1.3428	1.2858	-0.3098
150.0	-1.2364	0.0349	0.3021	0.5740	0.8373	1.0277	1.2808	1.4338	1.5273	1.5558	1.5190	-0.3175
160.0	-1.3115	-0.0756	0.2027	0.4946	0.7874	1.0055	1.3119	1.5101	1.6462	1.7104	1.6986	-0.3114
170.0	-1.3567	-0.1686	0.1108	0.4102	0.7180	1.0189	1.2949	1.5273	1.6988	1.7962	1.8118	-0.2866
180.0	-1.3717	-0.2394	0.0328	0.3282	0.6368	0.9447	1.2344	1.4867	1.6830	1.8077	1.8506	-0.2394
190.0	-1.3567	-0.2866	-0.0281	0.2564	0.5500	0.8495	1.1364	1.3930	1.6012	1.7448	1.8118	-0.1686
200.0	-1.3115	-0.3114	-0.0719	0.1877	0.4612	0.7488	1.0080	1.2538	1.4603	1.6126	1.6985	-0.0756
210.0	-1.2364	-0.3175	-0.1015	0.1299	0.3716	0.6167	0.8558	1.0778	1.2703	1.4210	1.5189	0.0349
220.0	-1.1312	-0.3097	-0.1215	0.0766	0.2805	0.4856	0.6860	0.8746	1.0433	1.1832	1.2856	0.1552
230.0	-0.9958	-0.2938	-0.1376	0.0236	0.1859	0.3469	0.5068	0.6534	0.7919	0.9140	1.0139	0.2756
240.0	-0.8300	-0.2750	-0.1542	-0.0333	0.0855	0.2016	0.3137	0.4229	0.5282	0.6283	0.7200	0.3849
250.0	-0.6336	-0.2581	-0.1762	-0.0972	-0.0220	0.0498	0.1198	0.1902	0.2630	0.3395	0.4192	0.4724
260.0	-0.4076	-0.2464	-0.2060	-0.1694	-0.1064	-0.1055	-0.0739	-0.0382	0.0051	0.0590	0.1248	0.5289
270.0	-0.1531	-0.2423	-0.2442	-0.2492	-0.2560	-0.2619	-0.2635	-0.2572	-0.2388	-0.2049	-0.1531	0.5485
280.0	0.1248	-0.2464	-0.2899	-0.3343	-0.3772	-0.4151	-0.4446	-0.4620	-0.4637	-0.4463	-0.4074	0.5289
290.0	0.4193	-0.2581	-0.3406	-0.4209	-0.4954	-0.5605	-0.6128	-0.6489	-0.6661	-0.6617	-0.6337	0.4724
300.0	0.7201	-0.2751	-0.3930	-0.5045	-0.6058	-0.6932	-0.7636	-0.8144	-0.8435	-0.8492	-0.8301	0.3850
310.0	1.0140	-0.2938	-0.4427	-0.5804	-0.7065	-0.8087	-0.8935	-0.9558	-0.9943	-1.0079	-0.9959	0.2757
320.0	1.2857	-0.3098	-0.4849	-0.6439	-0.7841	-0.9032	-0.9996	-1.0709	-1.1171	-1.1373	-1.1313	0.1556
330.0	1.5190	-0.3175	-0.5146	-0.6907	-0.8448	-0.9741	-1.0790	-1.1582	-1.2111	-1.2372	-1.2364	0.0349
340.0	1.6985	-0.3114	-0.5270	-0.7171	-0.8812	-1.0193	-1.1316	-1.2170	-1.2758	-1.3074	-1.3116	-0.0756
350.0	1.8118	-0.2866	-0.5175	-0.7195	-0.8925	-1.0376	-1.1556	-1.2467	-1.3108	-1.3476	-1.3567	-0.1685
360.0	1.8506	-0.2394	-0.4827	-0.6949	-0.8762	-1.0279	-1.1512	-1.2473	-1.3162	-1.3578	-1.3717	-0.2394
HEIGHT =	3.2223	0.8659	1.1084	1.4079	1.7521	2.1154	2.4675	2.7745	3.0150	3.1656	3.2223	0.8659

REFK1 = 0.5764 REFK2 = 0.5764 REFK3 = 0.5764